

Journal Pre-proof

Pyrido[2, 3-*d*]pyrimidin-7(8*H*)-ones as New Selective Orally Bioavailable Threonine Tyrosine Kinase (TTK) Inhibitors

Minhao Huang, Yongjun Huang, Jing Guo, Lei Yu, Yu Chang, Xiaolu Wang, Jinfeng Luo, Yanhui Huang, Zhengchao Tu, Xiaoyun Lu, Yong Xu, Zhimin Zhang, Zhang Zhang, Ke Ding

PII: S0223-5234(20)30995-8

DOI: <https://doi.org/10.1016/j.ejmech.2020.113023>

Reference: EJMECH 113023

To appear in: *European Journal of Medicinal Chemistry*

Received Date: 20 March 2020

Revised Date: 8 May 2020

Accepted Date: 10 November 2020

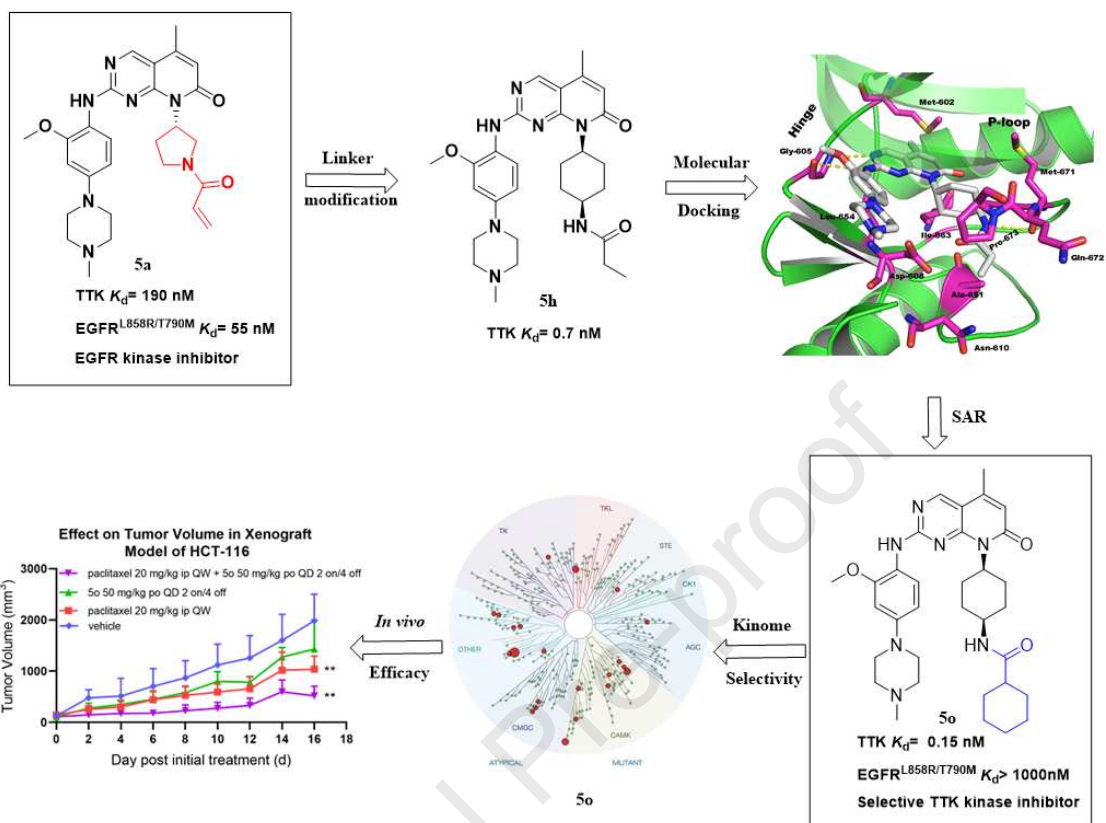
Please cite this article as: M. Huang, Y. Huang, J. Guo, L. Yu, Y. Chang, X. Wang, J. Luo, Y. Huang, Z. Tu, X. Lu, Y. Xu, Z. Zhang, Z. Zhang, K. Ding, Pyrido[2, 3-*d*]pyrimidin-7(8*H*)-ones as New Selective Orally Bioavailable Threonine Tyrosine Kinase (TTK) Inhibitors, *European Journal of Medicinal Chemistry*, <https://doi.org/10.1016/j.ejmech.2020.113023>.

This is a PDF file of an article that has undergone enhancements after acceptance, such as the addition of a cover page and metadata, and formatting for readability, but it is not yet the definitive version of record. This version will undergo additional copyediting, typesetting and review before it is published in its final form, but we are providing this version to give early visibility of the article. Please note that, during the production process, errors may be discovered which could affect the content, and all legal disclaimers that apply to the journal pertain.

© 2020 Published by Elsevier Masson SAS.



Graphical Abstract



Pyrido[2, 3-*d*]pyrimidin-7(8*H*)-ones as New Selective Orally Bioavailable Threonine Tyrosine Kinase (TTK) Inhibitors

Minhao Huang,^{†,‡,§,#} Yongjun Huang,^{Ψ,#} Jing Guo,^{Ψ,#} Lei Yu,[†] Yu Chang,^Ψ Xiaolu Wang,^Ψ
Jinfeng Luo,^{†,§} Yanhui Huang,^{†,§} Zhengchao Tu,^{†,§} Xiaoyun Lu,^Ψ Yong Xu,^{†,§} Zhimin
Zhang,^{Ψ,*} Zhang Zhang,^{Ψ,*} Ke Ding^{Ψ,*}

[†]Guangdong Provincial Key Laboratory of Biocomputing, Joint School of Life Sciences, Guangzhou Institutes of Biomedicine and Health, Chinese Academy of Sciences; Guangzhou Medical University, Guangzhou 510530, China

[‡]University of Chinese Academy of Sciences, No. 19 Yuquan Road, Beijing 100049, China

[§]Guangzhou Regenerative Medicine and Health Guangdong Laboratory (GRMH-GDL), Guangzhou 510530, China

^ΨInternational Cooperative Laboratory of Traditional Chinese Medicine Modernization and Innovative Drug Discovery of Chinese Ministry of Education (MOE), Guangzhou City Key Laboratory of Precision Chemical Drug Development, School of Pharmacy, Jinan University, 601 Huangpu Avenue West, Guangzhou 510632, China

[#]These authors contributed equally.

*Corresponding authors, E-mail: zhangzm@jnu.edu.cn (Zhimin Zhang), 601 Huangpu Avenue West, Guangzhou 510632, China; zhang_zhang@jnu.edu.cn (Zhang Zhang), 601 Huangpu Avenue West, Guangzhou 510632, China; dingke@jnu.edu.cn (Ke Ding), 601 Huangpu Avenue West, Guangzhou 510632, China.

KEYWORD: Pyrido[2,3-*d*]pyrimidin-7(8*H*)-ones, threonine tyrosine kinase (TTK), orally bioavailable, inhibitor

ABSTRACT: A series of pyrido[2, 3-*d*]pyrimidin-7(8*H*)-ones were designed and synthesized as new selective orally bioavailable Threonine Tyrosine Kinase (TTK) inhibitors. One of the representative compounds, **5o**, exhibited strong binding affinity with a K_d value of 0.15 nM, but was significantly less potent against a panel of 402 wild-type kinases at 100 nM. The compound also potently inhibited the kinase activity of TTK with an IC_{50} value of 23 nM, induced chromosome missegregation and aneuploidy, and suppressed proliferation of a panel of human cancer cell lines with low μ M IC_{50} values. Compound **5o** demonstrated good oral pharmacokinetic properties with a bioavailability value of 45.3% when administered at a dose of 25 mg/kg in rats. Moreover, a combination therapy of **5o** with paclitaxel displayed promising *in vivo* efficacy against the HCT-116 human colon cancer xenograft model in nude mice with a Tumor Growth Inhibition (TGI) value of 78%. Inhibitor **5o** may provide a new research tool for further validating therapeutic potential of TTK inhibition.

INTRODUCTION

Threonine tyrosine kinase (TTK, also known as Monopolar Spindle 1, Mps1) is a dual-specificity protein kinase which was first discovered in budding yeast in the early 1990s [1]. TTK has been identified as a core component of the spindle assembly checkpoint (SAC) and plays a crucial role in accurate separation of sister chromatids during mitosis to avoid aneuploidy [2-4]. TTK is essential for the activation and maintenance of SAC functions. Upon recruitment by Aurora B to unattached kinetochore,

TTK phosphorylates kinetochore null protein 1 (Knl1) and consequently forms a tetrameric mitotic checkpoint complex (MCC). MCC inhibits anaphase promoting complex (APC/C) to restrain chromosome segregation and mitotic exit and prevents premature initiation of anaphase [2, 5-8]. In addition to its role in mitosis, TTK is also heavily involved in centrosome duplication [8-11], DNA damage checkpoint response [12-16], ciliogenesis [17], meiosis [18, 19], cell transformation and chromosomal instability (CIN) [20].

TTK was identified as one of the top 25 overexpressed genes in a variety of human cancers [21]. For instance, elevated levels of TTK have been frequently detected in colon cancer [22, 23], breast cancer including TNBC (triple-negative breast cancer) [24-27], ovarian cancer [28], hepatocellular carcinoma [29-31], bladder cancer [32], pancreatic cancer [33] and glioblastoma [34-36], and is closely associated with poor prognosis of these diseases. TTK mediated aneuploidy is a hallmark of 70% – 95% of human cancer cells in the top 10 most commonly affected organs [37]. Selective knockdown of TTK by siRNA led to apoptosis of breast cancer cells with high aneuploidy levels while not obviously affecting nonmalignant cells [27]. The cytotoxic differentiation between tumor and normal cells implies that TTK inhibition could be considered as a new attractive wide-spectrum strategy for cancer therapy.

A number of TTK inhibitors with different kinome selectivity profiles have been reported from both pharmaceutical companies and academic institutes [38-44]. At least 5 molecules have been advanced to Phase I or II clinical investigation, including S-81694 (structure undisclosed), BAY-1161909 (**1**) [45, 46], BAY-1217389 (**2**) [45, 46],

CFI-402257 (**3**) [47] and BOS-172722 (**4**) [48] (Figure 1). Both inhibitors **1** and **2** were developed from Bayer AG. The compounds exhibited single digit nM IC₅₀ values against TTK when assayed at high ATP concentrations, and potently suppressed the proliferation of HeLa cervix carcinoma cells with IC₅₀ values of 260 and 7.6 nM, respectively. However, they only displayed moderate monotherapy efficacy with tumor growth inhibition rates (TGI) less than 50% in various mouse tumor models possibly due to their limited tolerability [46]. However, significant *in vivo* antitumor efficacy was achieved by combining the inhibitors with paclitaxel, [45, 46] and both compounds have been advanced to Phase I clinical trial in combination with intravenous paclitaxel (NCT02138812, NCT02366949). Compound **3** is another highly potent and selective TTK inhibitor with low nM IC₅₀ potency inhibiting TTK kinase. This compound strongly suppresses proliferation of MDA-MB-468, HCT-116 and OVCAR-3 cancer cells with IC₅₀ values of 2.0, 2.0 and 4.0 nM, respectively, and demonstrated a TGI value of 68% following daily oral dosing of 6.5 mg/kg/day in a xenograft model of HCT-116 cancer cells as a single-agent treatment [47]. Clinical efficacy of **3** as a monotherapy is being actively investigated in patients with advanced solid tumors (NCT02792465). Another promising TTK inhibitor **4** is currently in a Phase 1/1b clinical trial in combination with paclitaxel. The compound exhibited an IC₅₀ value of 11 nM and displayed extraordinary kinome selectivity against a panel of more than 400 kinases [48]. Despite encouraging progress on TTK inhibitor development, no clinical data has been disclosed to date. It is still highly desirable to identify new selective TTK inhibitors with differentiated chemical structures and good selectivity profiles to further validate TTK as a therapeutic target.

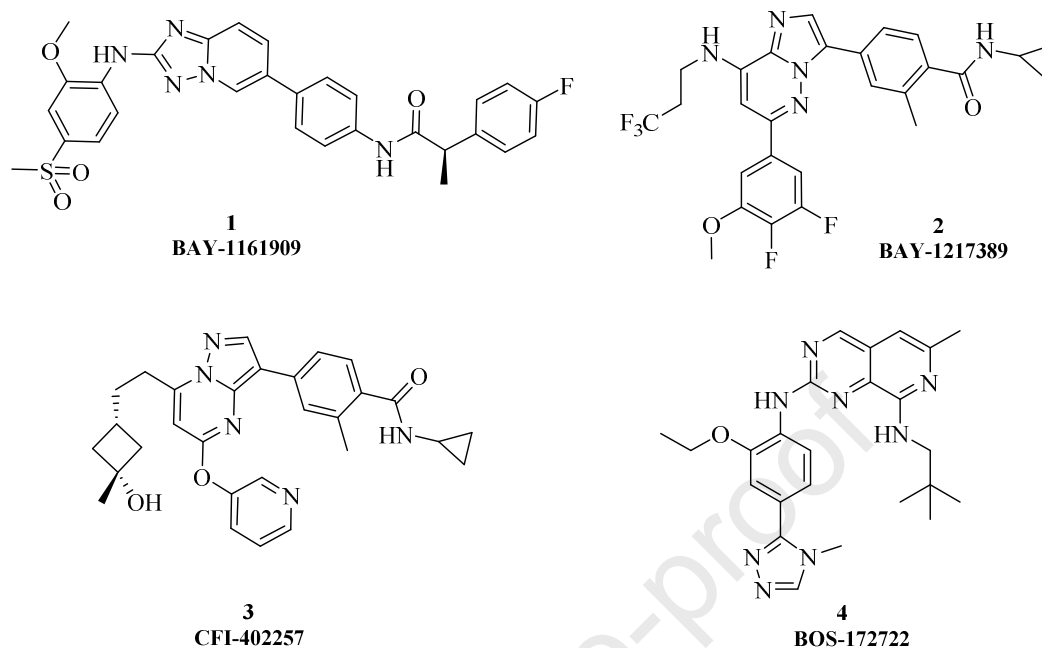


Figure 1. Chemical structures of the clinically investigated TTK inhibitors.

Herein, we report our efforts to discover pyrido[2, 3-*d*]pyrimidin-7(8*H*)-ones as new orally bioavailable selective TTK inhibitors.

MOLECULAR DESIGN

Compound **5a** is a covalent EGFR^{L858R/T790M} inhibitor with an IC₅₀ value of 91.8 nM discovered in our laboratory [49]. Kinome selectivity investigations revealed that this compound exhibited moderate TTK binding affinity with a *K_d* value of 190 nM. Since compounds with a pyrido[2, 3-*d*]pyrimidin-7(8*H*)-one scaffold tend to exhibit a good kinase selectivity [50], we utilized **5a** as an initial lead compound for new selective TTK inhibitor discovery.

A preliminary computational study suggested that compound **5a** could bind to the ATP binding site of TTK with a similar “U-shaped” configuration to that of EGFR in a type-I binding mode (Figure 2). The aminopyrimidine moiety of compound **5a** interacts with

Gly605 or Met793 at the hinge region of TTK or EGFR, respectively, through a classical bidentate hydrogen bonding network. A hydrophobic sandwich of the pyrido[2,3-*d*]pyrimidin-7(8*H*)-one scaffold with a ceiling Ala551 residue and a floor consisted of Leu654 and Ile663 is formed to stabilize binding of the molecule with TTK protein. These interactions are similar to those formed with the Ala743 and Leu844 residues of EGFR. The hydrophilic phenylpiperazine moiety is exposed to a solvent accessible surface, which might only slightly influence the binding affinity. While the acrylamide of **5a** forms a covalent bond with Cys797 of EGFR, it instead remains close to Ala651 and Asp608 of TTK. The acrylamide moiety may also form hydrophobic interactions with the surrounding residues (Val678, Ile663, Pro673 and Leu654) in the flexible loop of the TTK protein. Based on these observations, it was hypothesized that the acrylamide group in **5a** could be replaced by a saturated carboxyl amide to achieve potent and selective binding with TTK over EGFR.

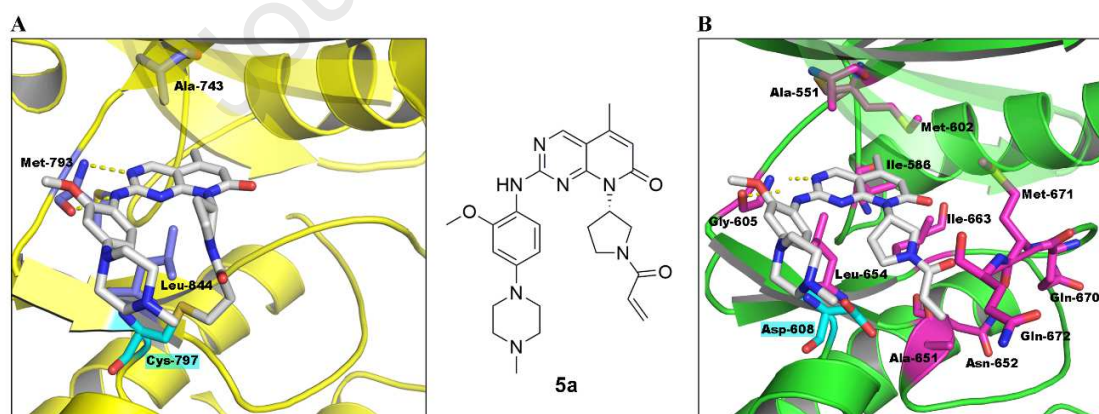


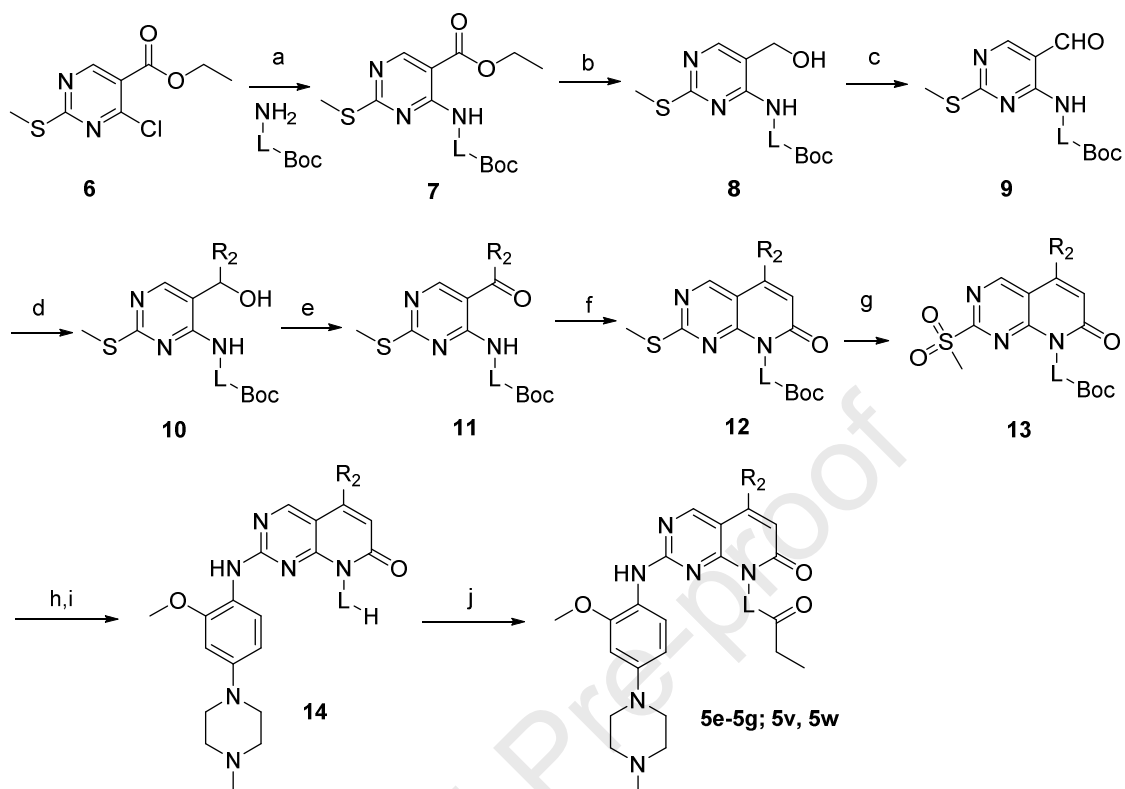
Figure 2. Predicted binding modes of compound **5a** in EGFR^{L858R/T790M} and TTK. (A) Predicted binding mode of **5a** with EGFR^{L858R/T790M} kinase (PDB code: 5GMP); (B) Predicted binding pose of **5a** with TTK kinase (PDB code: 5EH0). The ligand is shown in

a gray stick representation.

CHEMISTRY

Synthesis of the designed pyrido [2, 3-*d*] pyrimidin-7(8*H*)-ones is outlined in Scheme 1 and Scheme 2. Briefly, commercially purchased ethyl 4-chloro-2-(methylthio)pyrimidine-5-carboxylate (**6**) was reacted with different Boc-protected aliphatic amines to generate intermediates **7**, which were then reduced by lithium aluminum hydride (LiAlH₄) to yield alcohols **8**. Compounds **8** were oxidized by manganese dioxide (MnO₂) to produce aldehydes **9**. Compounds **9** were reacted with different Grignard reagents to yield intermediates **10** which were then oxidized to give derivatives **11**. The key intermediates **12** were prepared by a tandem condensation-cyclization of **11** with (2-methoxy-2-oxoethylidene) triphenylphosphorane. With intermediates **12** in hand, the designed molecules **5e-5g**, **5v** and **5w** were readily prepared by following previously reported methods [51].

Scheme 1. Synthesis of compounds **5e-5g**, **5v** and **5w**^a

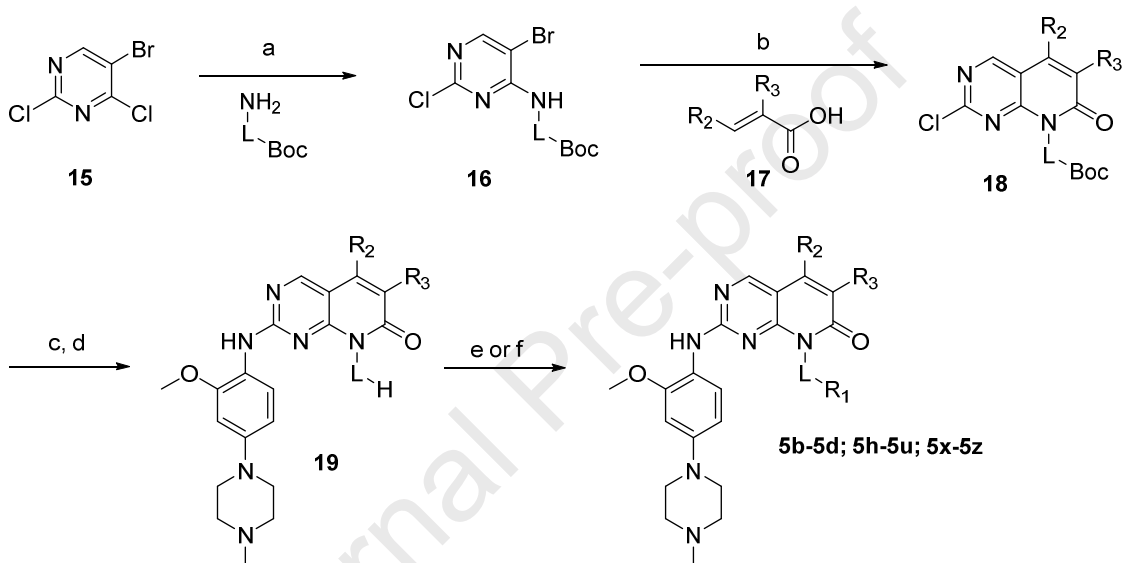


Reagents and conditions: (a) K₂CO₃ (2.0 eq.), MeCN, 0 °C to rt, 75-90%; (b) LiAlH₄ (2.0 eq.), tetrahydrofuran (THF), -40 °C to 0 °C, 45-55%; (c) MnO₂ (10.0 eq.), dichloromethane (DCM), rt, 80-95%; (d) Grignard reagent (2.0 eq.), THF, -78 °C, argon, 45-70%; (e) MnO₂ (10.0 eq.), DCM, rt, 75-90%; (f) (2-Methoxy-2-oxoethylidene) triphenylphosphorane (1.5 eq.), toluene, 110 °C, argon, 2 d, 18-35%; (g) 3-Chloroperoxybenzoic acid (*m*-CPBA) (3.0 eq.), DCM, 0 °C, 3.0 hrs, 80-96%; (h) 2-methoxy-4-(4-methylpiperazin-1-yl) aniline (1.1 eq.), trifluoroacetic acid (TFA) (1.2 eq.), 2-Butanol (2-BuOH), 95 °C, argon, 18 hrs; (i) TFA (10.0 eq.), DCM, rt, 2 hrs, 20-35% for two steps; (j) propionyl chloride (1.1 eq.), *N,N*-Diisopropylethylamine (DIEA) (1.2 eq.), DCM, 0 °C, 30 minutes, 50-83%.

Alternatively, commercially available 5-bromo-2, 4-dichloropyrimidine (**15**) was

reacted with different Boc-protected aliphatic amines to generate intermediates **16** which were reacted with various acrylic acids **17** under palladium-catalyzed conditions to produce derivatives **18**. Using **18** as the key intermediates, compounds **5b-5d**, **5h-5u** and **5x-5z** were prepared by following similar procedures to the previous protocols [49].

Scheme 2. Synthesis of compounds **5b-5d**, **5h-5u** and **5x-5z**^a



^a**Reagents and conditions:** (a) K_2CO_3 (2.0 eq.), MeCN, 0 °C to rt, 75-96%; (b) two steps, 1) α,β -unsaturated carboxylic acid (5.0 eq.), DIEA (10.0 eq.), bis(benzonitrile) palladium (II) dichloride (0.05 eq.), tri-*o*-tolylphosphine (0.05 eq.), anhydrous THF, 70 °C, argon, 16 hrs; 2) Ac_2O (0.3 eq.), 90 °C, argon, 24 hrs, 32-60% for two steps; (c) 2-methoxy-4-(4-methylpiperazin-1-yl) aniline (1.1 eq.), TFA (1.2 eq.), 2-BuOH, 95 °C, argon, 18 hrs; (d) TFA (10.0 eq.), DCM, rt, 2 hrs, 33-40% for two steps; (e) R_1OH (1.3 eq.), 2-(7-aza-1H-benzotriazol-1-yl)-1,1,3,3-tetramethyluronium hexafluorophosphate (HATU) (1.2 eq.), DIEA (1.5 eq.), *N,N*-Dimethylformamide (DMF), rt, 2 hrs, 60-80%; (f) R_1Cl (1.1 eq.), DIEA (1.2 eq.), DCM, 0 °C, 30 minutes, 56-90%.

RESULT AND DISCUSSION

Based on preliminary computational investigation, the acrylamide moiety of compound **5a** was first saturated to yield the corresponding propionamide **5b** to prevent Michael reaction with EGFR or other proteins containing similarly positioned cysteine residues. Given the technical difficulties in determining TTK kinase inhibitory activity [52], the binding affinity of the novel compounds was primarily evaluated by utilizing an active site-directed competition binding assay (conducted by Eurofins DiscoveryX Corporation, San Diego, CA, USA) to guide the structural optimization [53]. Inhibitor **3** was utilized as a positive reference compound and exhibited a binding constant K_d value of 0.071 nM (Table 1). Highly consistent with our predictions, compound **5b** exhibited a similar TTK binding affinity to that of compound **5a** with a K_d value of 145 nM, while its potency against EGFR was significantly decreased ($K_d > 1000$ nM). Utilizing compound **5b** as a lead molecule, new compounds were designed and synthesized by replacing the pyrrolidinyl linker moiety with a variety of heterocyclic groups (**5c-5i**). This confirmed that the linker group had significant impact on TTK binding activity (Table 1). Although replacement of the *S*-pyrrolidinyl linker with its *R*- isomer (**5d**) only caused a 2-fold loss of potency, an azetidiny substitution (**5c**) demonstrated almost totally abolished TTK binding potency. The 4-piperidyl linked molecule (**5g**) exhibited strong binding with TTK with a K_d value of 9.3 nM, but the *R*- (**5e**) or *S*- (**5f**) 3-piperidyl substituted molecules were approximately 27 and 21 fold less potent, respectively. Encouragingly, when a *cis*- (**5h**) or *trans*- (**5i**) 4-amino-cyclohexyl linker was introduced, the resulting compounds tightly bound TTK with K_d values of 0.71 nM and 2.8 nM, respectively.

A computation study was also conducted to rationalize the diverse impacts of the different linkers on the TTK binding affinity (Figure 3 and Supporting Information Figure S1). It was shown that the three more potent molecules, i.e. **5g**, **5h** and **5i**, demonstrated overall similar binding poses to that of compound **5b** (Figure 3). However, the increased volume of the linkers present in **5g**, **5h** and **5i** may favor improved hydrophobic interactions with Ala651, Met671 and Pro673, when compared to those of **5b**. It was also shown that compounds with *S*-pyrrolidinyl (**5b**) and 3-piperidyl (**5f**) linkers would achieve a better fit into the hydrophobic sandwich consisting of Ala651 and Met671 in TTK (Supporting Information Figure S1). Alternately, steric conflict was observed between **5c** and Pro673 of TTK, which may explain its significant loss of binding affinity (Supporting Information Figure S1B). Additionally, hydrogen-bond interaction networks were also observed between the carboxyl amide of the inhibitors and TTK. For instance, the propionamide moiety of **5h** was sandwiched between Met671 and Ala651 to form strong hydrogen-bond interactions that benefit binding with TTK, while only one hydrogen bond could form in this region for compounds **5g** or **5i**. The computational study further suggested that the ethyl moiety in **5h** is located in a hydrophobic cavity formed by Asn652, Ile663, Gln670, Met671, Pro673 and Val678 in the loop region, and that a hydrophobic group with increased size could be accommodated in this pocket to potentially improve binding affinity further. Thus, several new molecules with different hydrophobic tails (**5j-5r**) were designed and synthesized. The results showed that while the acetyl analog **5j** demonstrated similar potency to that of **5h**, compounds with larger hydrophobic groups indeed exhibited improved binding affinities with TTK. For instance,

the cyclopropyl (**5k**), *iso*-propyl (**5l**), and phenyl (**5q**) substituted compounds displayed improved binding affinities with K_d values of 0.41, 0.50 and 0.30 nM, respectively. Significantly, compounds with *tert*-butyl (**5m**), cyclopentyl (**5n**) and cyclohexanyl (**5o**) substituents exhibited the strongest affinity with K_d values of 0.20, 0.12 and 0.15 nM, respectively. It was also noteworthy that this position was able to accommodate large hydrophobic groups such as adamantyl (**5p**) or 1-naphthyl (**5r**) substituents (K_d values of 0.56 and 1.1 nM, respectively). We have predicted that the carbonyl group in the alkyl amide moiety could form a hydrogen bond with Met671 (Figure 3) improving binding with TTK, consistent with this removal of the carbonyl group in **5k** (to give **5s**) caused an approximate 15-fold loss of potency (**5s** exhibited a K_d value of 6.1 nM). Per-residue binding free energy decomposition clearly suggested that the predicted hot-spot residues (i.e., Asn654, Pro673 and Val678 in loop region) contributed greatly to the binding of **5o** with TTK (Supporting Information, Figure S2).

The Structure-Activity Relationship (SAR) investigation also revealed that the 2'-position in the west phenyl ring favors hydrophobic group substitution. For instance, the 2'-methoxyl (**5h**) and 2'-methyl (**5ha**) derivatives exhibited TTK binding affinity with K_d values of 0.71 and 0.63 nM, respectively. Whereas, the corresponding 3'-substituted molecules **5hb** and **5hc** were 6-fold less potent (K_d values of 4.2 and 3.9 nM, respectively). Our computational investigation suggested that additional interactions of the 2'-methoxyl or 2'-methyl group with Cys604 and Gln541 residues of TTK may contribute to the improved potencies of **5h** and **5ha** (Supporting Information, Figure S3).

Our previous studies have suggested that a hydrophobic substituent at the 5-position of

the pyrido[2, 3-*d*]pyrimidin-7(8*H*)-one ring system could contribute greatly to the target specificity of the compounds, although it might be detrimental to a compound's potency [50]. Similar to previous observations [54], removal of the 5-methyl group in **5h** resulted in a 2-fold potency improvement (**5t**). However, when the 5-methyl group was replaced by an ethyl (**5u**) or cyclopropyl (**5v**) group, the resulting molecules exhibited 2- and 11-fold less potency, respectively. Most notable, the 5-phenyl compound (**5w**) displayed a K_d value of 825 nM, which was approximately 1162-fold less potent than compound **5h**. Interestingly, the 5-methyl group of **5h** could be moved to the 6- position to provide a 3-fold potency improvement (**5x**). The corresponding cyclopentanecarbonyl and cyclohexanecarbonyl substituted derivatives **5y** and **5z** also exhibited similar binding potency to that of **5n** and **5o**, with K_d values of 0.17 and 0.16 nM, respectively.

Kinase inhibitory activity of selected compounds was further determined by utilizing a direct filter-binding radiometric kinase activity assay to validate their TTK inhibitory potency (conducted by Eurofins Cerep SA, France) (Table 2). Compounds **5n**, **5o**, **5y** and **5z** exhibited strong TTK kinase inhibition with IC_{50} values of 19, 23, 11 and 20 nM, respectively, which were comparable to that of compound **3** (IC_{50} , 17 nM). Highly consistent with the measured weaker binding affinities of compounds **5v** and **5b** they also displayed poorer kinase inhibitory activities with IC_{50} values of 50 and >1000 nM, respectively. Collectively, compounds **5n**, **5o**, **5y** and **5z** represented the most potent TTK inhibitors in this series displaying comparable potency to that of the clinical candidate compound **3**.

Table 1. Binding affinity of compounds **5a-5z** and **5ha-5hc** against TTK^a

R₄ = 2-OMe: 5a-5z; 2-Me: 5ha; 3-OMe: 5hb, 3-Me: 5hc

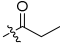
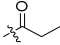
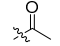
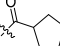
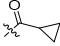
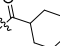
L:

I	II	III	IV	V	VI	VII	VIII

TTK

K_d value (nM)

Compd.	L	R ₁	R ₂	R ₃	K _d value of TTK (nM)	Compd.	L	R ₁	R ₂	R ₃	K _d value of TTK (nM)
3	-	-	-	-	0.071 (0.072, 0.070)	5l	□		Me	H	0.50 (0.46, 0.54)
5a	□		Me	H	190 (180, 200)	5m	□		Me	H	0.20 (0.21, 0.18)
5b	□		Me	H	145 (160, 130)	5n	□		Me	H	0.12 (0.11, 0.12)
5c	□		Me	H	>1000 (>1000, >1000)	5o	□		Me	H	0.15 (0.13, 0.17)
5d	□		Me	H	310 (280, 330)	5p	□		Me	H	0.56 (0.61, 0.51)
5e	□		Me	H	250 (240, 260)	5q	□		Me	H	0.30 (0.26, 0.34)
5f	□		Me	H	200 (160, 240)	5r	□		Me	H	1.1 (0.75, 1.5)
5g	□		Me	H	9.3 (8.8, 9.8)	5s	□		Me	H	6.1 (5.4, 6.8)
5h	□		Me	H	0.71 (0.61, 0.80)	5t	□		H	H	0.41 (0.47, 0.34)
5i	□		Me	H	2.8 (2.8, 2.8)	5u	□		Et	H	1.5 (1.4, 1.5)
5ha	□		Me	H	0.63 (0.57, 0.69)	5v	□		cycli c-Pr	H	7.9 (6.5, 9.3)
5hb	□		Me	H	4.2 (3.6, 4.8)	5w	□		Ph	H	825 (870, 780)

5hc		Me	H	3.9 (3.7, 4.0)	5x		H	Me	0.29 (0.32, 0.25)
5j		Me	H	0.72 (0.66, 0.78)	5y		H	Me	0.17 (0.19, 0.15)
5k		Me	H	0.41 (0.45, 0.36)	5z		H	Me	0.17 (0.2, 0.13)

^aThe binding affinity (K_d) was determined by utilizing an active site-directed competition binding assay (conducted by Eurofins DiscoveryX Corporation, San Diego, CA, USA). The data is the mean from two independent experiments. The independent values are presented in the brackets.

Table 2. *In vitro* TTK Kinase Inhibition of the selected compounds ^a

Compd.	3	5b	5n	5o	5v	5y	5z
IC ₅₀ (nM)	17	>1000	19	23	50	11	20
	(17, 17)	(>1000, >1000)	(17, 20)	(21, 24)	(52, 48)	(12, 9)	(21, 18)

^aThe isolated enzyme inhibitory potency (IC₅₀) was determined by utilizing a direct filter-binding radiometric kinase activity assay (conducted by Eurofins Cerep SA, France). The data is the mean from two independent experiments. The independent values are presented in the brackets.

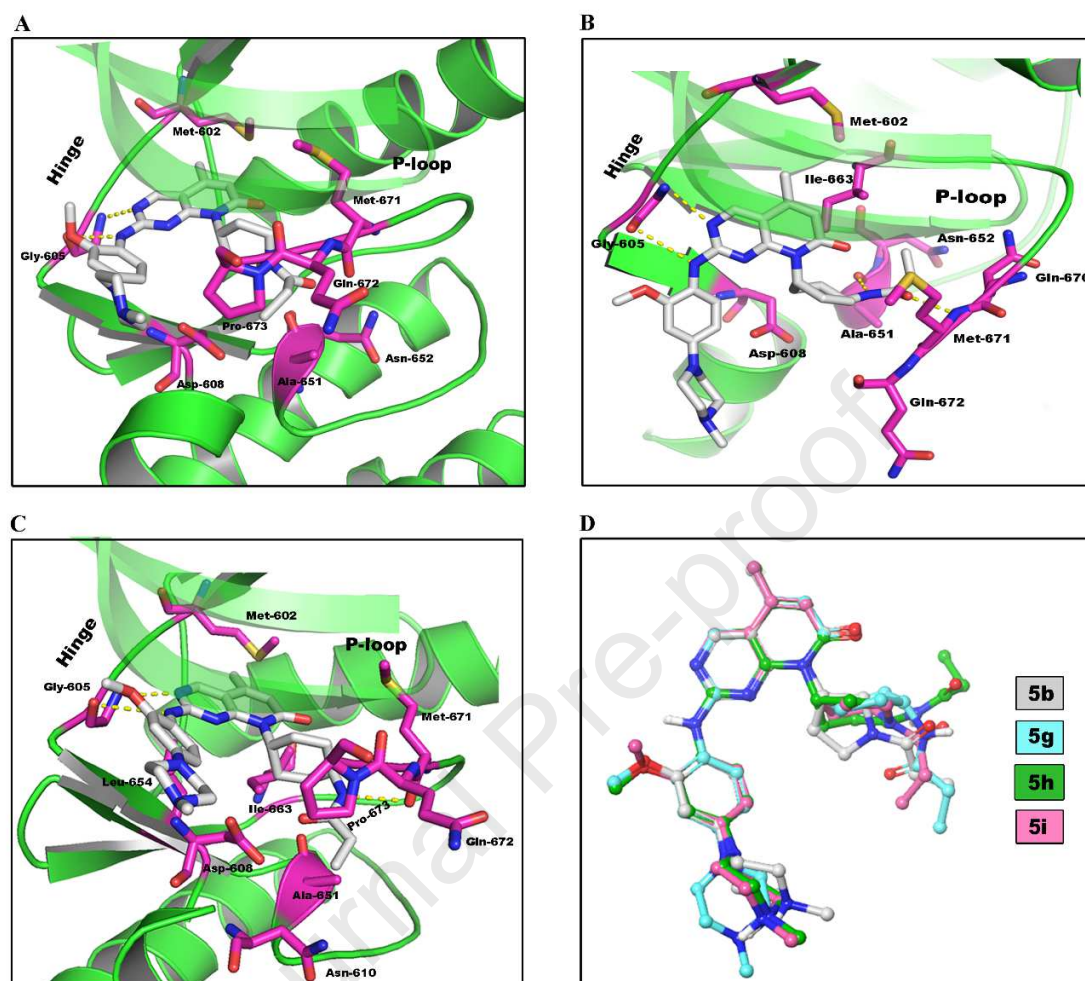


Figure 3. Representatives of the predicted binding modes of compounds **5g**, **5h** and **5i** in the active site of TTK (PDB code 5EH0). (A) The predicted binding mode of **5g** in TTK; (B) The predicted binding mode of **5h** in TTK; (C) The predicted binding mode of **5i** in TTK; (D) Superposition of compounds **5b**, **5g**, **5h** and **5i**.

The kinase selectivity of compounds **5o** and **5z** were also evaluated against a panel of 468 kinases (including 403 wild-type kinases) at a single concentration of 100 nM, which is over 600 times their respective K_d values against TTK. Only a small number of other kinases were inhibited by **5o**. 22 out of the 403 kinases exhibited more than 65%

inhibition at the tested concentration with **5** (i.e. DAPK3, IRAK1, MARK3, PIK3C2G and PIK3CD) displaying more than 90% inhibition (Table 3). The results also showed that **5z** exhibited relatively poorer kinome selectivity than **5o**. 47 potential off-target kinases (>65% inhibition) were identified with **19** showing more than 90% inhibition (Supporting Information Table S4). Further binding affinity determinations confirmed that **5o** bound with DAPK3 and MARK3 with K_d values of 13 and 11 nM, respectively, being 87- and 73- fold greater than that that observed for TTK, respectively (Table 3). However, compound **5o** did not show strong binding affinity with IRAK1, PIK3C2G and PIK3CD (K_d values > 1000 nM) as was initially suggested from the 100 nM single-concentration screen. These data collectively supported **5o** as a highly selective TTK inhibitor.

Table 3 Kinome selectivity profiles of **5o**^a

Target	%Inhibition	K_d (nM)	Target	%Inhibition	K_d (nM)
PIK3CD	100	>1000	TTK	98.1	0.15(0.13, 0.17)
DAPK3	94.5	13 (12, 13)	PIK3C2G	94.4	>1000
MARK3	92	11(11, 11)	IRAK1	91.8	>1000
JNK3	87	-	PHKG2	87	-
STK16	87	-	JNK2	86	-
DAPK1	85	-	ULK2	85	-
SNARK	84	-	DMPK	81	-
DCAMKL1	80	-	PIPK5	77	-
MELK	77	-	JNK1	75	-

STK39	75	-	GAK	70	-
CSNK2A1	69	-	ULK1	68	-
DAPK2	65	-			

^aKinome selectivity profile of compound **5o** against a panel of 468 kinases at a concentration of 100 nM. Kinases with > 65% inhibition are listed. K_d values of major potential “off-target” kinases for **5o** are also reported (conducted by Eurofins DiscoveryX Corporation, San Diego, CA, USA).

TTK is a kinetochore-associated kinase essential for vertebrate mitotic checkpoint death. TTK inhibition leads to impairment of SAC, and induces chromosome missegregation and aneuploidy [43, 55-58]. To examine the effect of compound **5o** on chromosome segregation, HCT-116 human colorectal cancer cells were treated with **5o** and the number of chromosome segregation errors present in mitotic cells was determined by immunostaining for centromeres (centromere protein B, CENP-B, green), spindle (β -tubulin, red) and nucleus (4',6-diamidino-2-phenylindole, DAPI, blue). Two less active inhibitors (i.e. **5c** and **5b**) and compound **3** were also included as the negative and positive controls, respectively. It was shown that treatment with **5o** (333.3 nM) caused an obvious increase in chromosome missegregations when compared to untreated cells (Figure 4A, 4B). SAC inactivation and gross chromosome segregation errors caused by **5o** had an impact on the cell cycle and survival of human cancer cells. Compound **5o** induced dose-dependent dysregulation of the cell cycle, resulting in an increase in the frequency of cells exhibiting aneuploid DNA content (Figure 4C). Compound **5o**-induced aneuploidy was accompanied by a progressive accumulation of apoptotic cells which

were detected by flow cytometry analysis (Figure 5E) after 48 hours of treatment. Western blot analysis also suggested that **5o** induced activation of apoptosis-related proteins, such as caspase 3, caspase 9 and poly ADP-ribose polymerase (PARP) (Figure 5D) in a dose-dependent manner. Phosphorylated histone H3, a biomarker for SAC over-ride and TTK inhibition [55, 58, 59], was also dose-dependently suppressed by **5o** (Figure 5D). Not surprisingly, the positive control **3** exhibited similar aneuploidy induction in HCT-116 human colorectal cancer cells as determined by the increase of aneuploid DNA content, while the target-inactive compounds **5b** and **5c** did not show any obvious effect (Supporting Information, Figure S4).

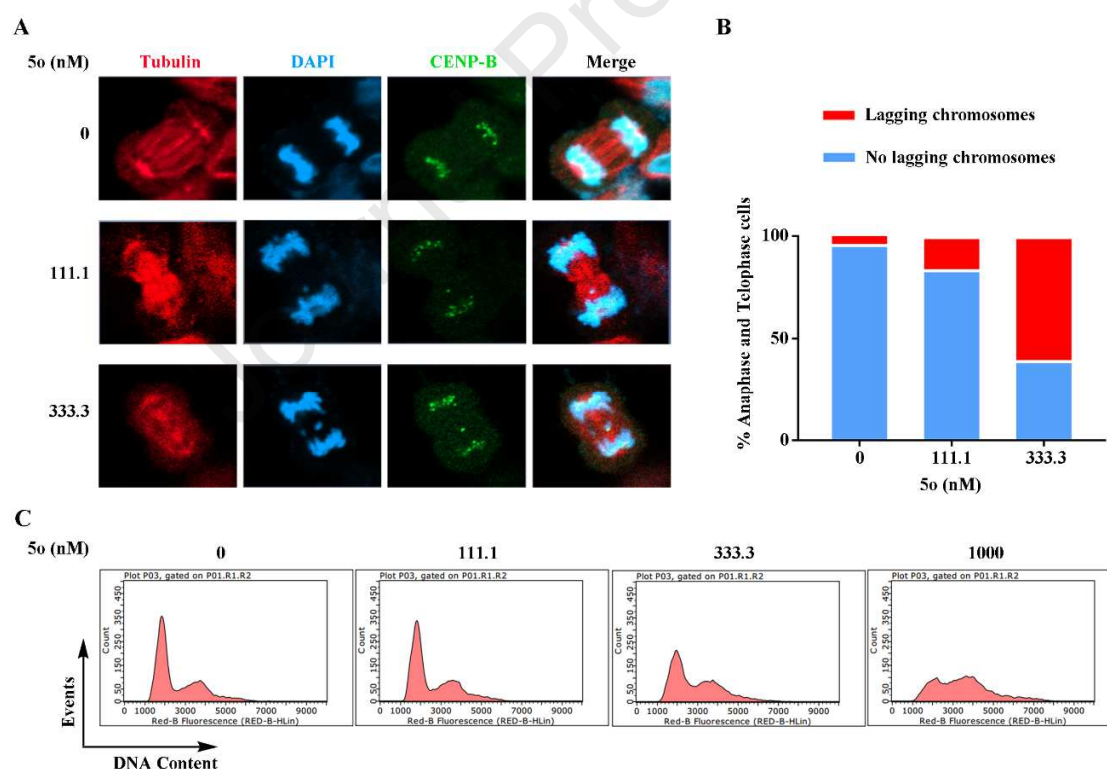


Figure 4. Compound **5o** inhibits the function of TTK in HCT-116 human colorectal cancer cells. (A) Compound **5o** causes aberrant chromosomal segregation in HCT-116

human colorectal cancer cells. Mitotic figures of HCT-116 human colorectal cancer cells treated with compound **5o** or DMSO for 24 hrs are displayed. Centromeres are stained in green, β -tubulin in red, and DAPI in blue; (B) Percentage of anaphase and telophase cells with lagging/ no lagging chromosomes (mean from two independent experiments, fifty cells were examined per treatment condition). Percentage of lagging chromosomes: DMSO: $3.8 \pm 1.1\%$; 111.1 nM compound **5o**: $16.1 \pm 4.6\%$; 333.3 nM compound **5o**: $60.6 \pm 1.9\%$; (C) Compound **5o** induces aneuploidy in HCT-116 human colorectal cancer cells. HCT-116 human colorectal cancer cells were treated with DMSO (control) or **5o** for 48 hrs. DNA content was assessed by flow cytometry.

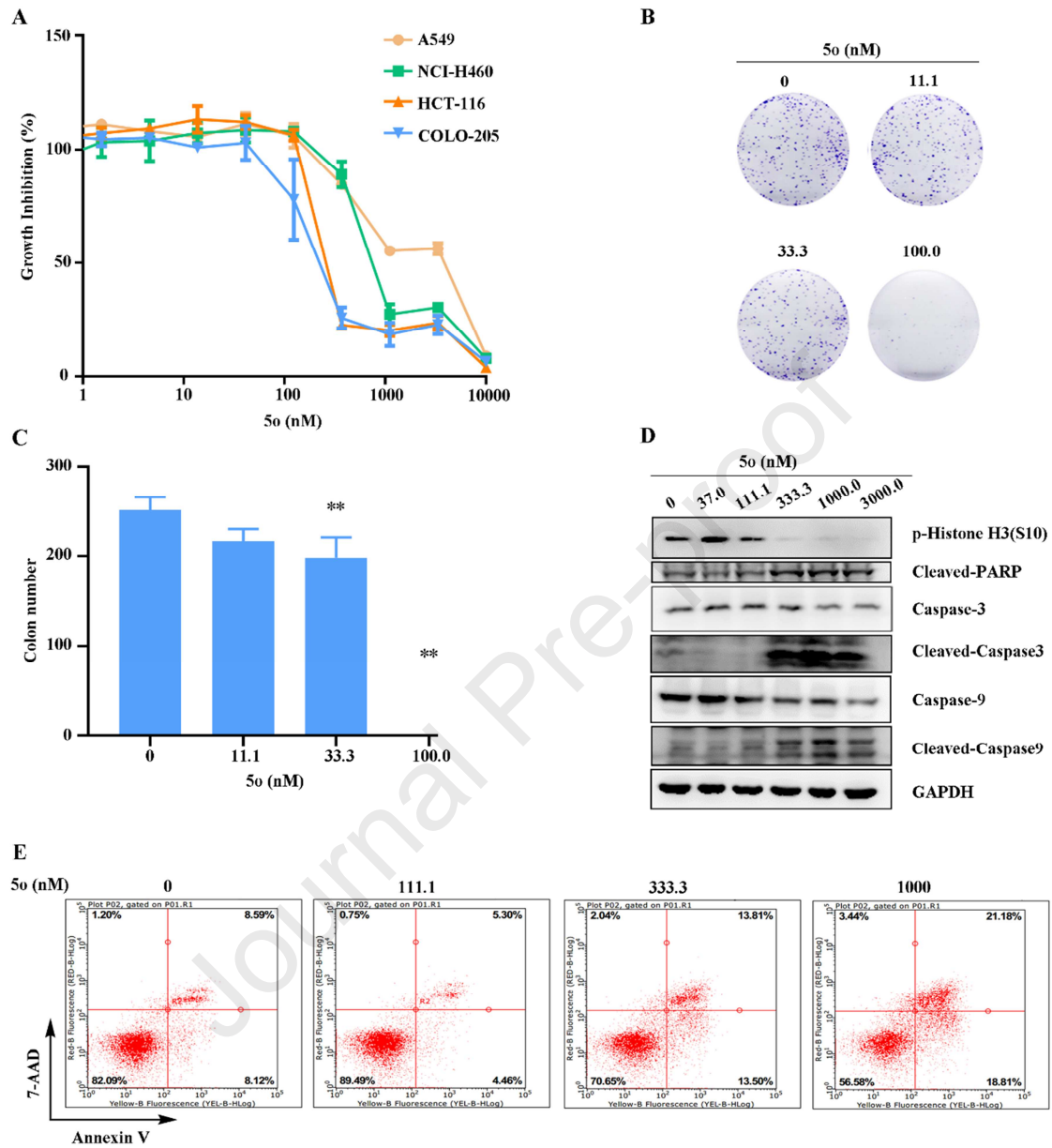


Figure 5. Effects of **5o** on proliferation and colony formation in cancer cells. (A) **5o** inhibits proliferation of cancer cells in vitro; (B) **5o** suppresses colony formation in HCT-116 human colorectal cancer cells. Cells were stained by crystal violet after treatment with DMSO (control) or **5o** for 7 days; (C) Colony numbers of assay were described in Figure 5B; (D) **5o** inhibits phosphorylation of histone H3 and activates

apoptosis-related proteins. HCT-116 human colorectal cancer cells were treated with DMSO (control) or **5o** for 48 hrs. Representative results were shown and similar results were obtained in other independent trials; (E) **5o** induced apoptosis in HCT-116 human colorectal cancer cells. HCT-116 human colorectal cancer cells were treated with DMSO (control) or **5o** for 48 hrs before DNA labeling by Annexin V and 7-AAD and cell apoptosis analysis by flow cytometry.

The anti-proliferative activity of **5o** against HCT-116 and COLO-205 human colorectal cancer cells, and A549 and NCI-H460 human lung cancer cells was also determined by using a Cell Counting Kit-8 (CCK-8) assay. It was shown that compound **5o** potently inhibits the growth of human cancer cells with IC₅₀ values of 0.41, 0.28, 4.40 and 1.09 μ M, respectively (Figure 5A, Supporting information, Table S1). Additionally, **5o** also exhibited moderate inhibition of HCT-116 human colorectal cancer cell colony formation (Figure 5B).

Pharmacokinetic parameters of the representative molecules **5o** and **5z** were also determined in SD rats to evaluate their drug-like properties (Table 4). It was shown that both compounds exhibited good pharmacokinetic properties with high plasma exposure (AUC), reasonable half-life ($T_{1/2}$) and acceptable oral bioavailability (F) values. For instance, compounds **5o** and **5z** demonstrated AUC_(0-∞) values of 13,021 and 33,346 (μ g/L)·h, $T_{1/2}$ values of 6.0 and 7.6 hrs, and oral bioavailability of 45.3% and 39.6%, respectively, at an oral dose of 25 mg/kg.

Table 4. Pharmacokinetic parameters of **5o** and **5z** in SD rats ^a

Com pd.	route	$T_{1/2}$ (h)	C_{max} (μ g/L)	AUC _(0-∞) (μ g/L)·h)	CLz (mL/h/kg)	F (%)
------------	-------	---------------	------------------------	---	---------------	-------

5o	IV (5 mg/kg)	3.58 ±0.03	2525.52 ±500.46	5307.22 ±449.55	946.43 ±76.46	
	PO (25mg/kg)	6.01 ±0.30	1228.70 ±63.51	13021.02 ±1419.37		45.25 ±4.76
5z	IV (5 mg/kg)	6.20 ±0.95	4739.97 ±733.38	15453.16 ±3580.87	336.79 ±86.06	
	PO (25 mg/kg)	7.62 ±0.75	2304.63 ±304.53	33346.28 ±2227.15		39.63 ±2.71

^aSD rat (male, three animals per group) weighing 190-230 g were used for the study.

In vivo efficacy of **5o** was further investigated as a single-agent and in combination with paclitaxel in a xenograft mouse model of HCT-116 cancer cells. CB17-SCID mice bearing HCT-116 tumor xenografts were treated with paclitaxel (20 mg/kg, intraperitoneal (ip), quaque week (QW)), **5o** (50 mg/kg, po, QD, 2 days on/4 days off) alone, or with a combination of paclitaxel (20 mg/kg, ip, QW) and **5o** (50 mg/kg, po, QD, 2 days on/4 days off), respectively. Compound **5o** or paclitaxel monotherapy exhibited moderate tumor growth inhibition with TGI values of 29% and 52%, respectively. Encouragingly, the combination strongly improved the *in vivo* efficacy with a TGI of 78%. This might be due to the fact that a TTK inhibitor could reduce paclitaxel-induced mitotic arrest and accelerate progression of cells through mitosis by weakening SAC activity, which will eventually lead to increased chromosomal segregation errors and cell death [46, 60, 61]. It is noteworthy that all treatment protocols were well tolerated with body weight loss values less than 15% and no significant damage to liver and kidney function observed (Figure 6C, 6D, Supporting information Table S2, Table S3).

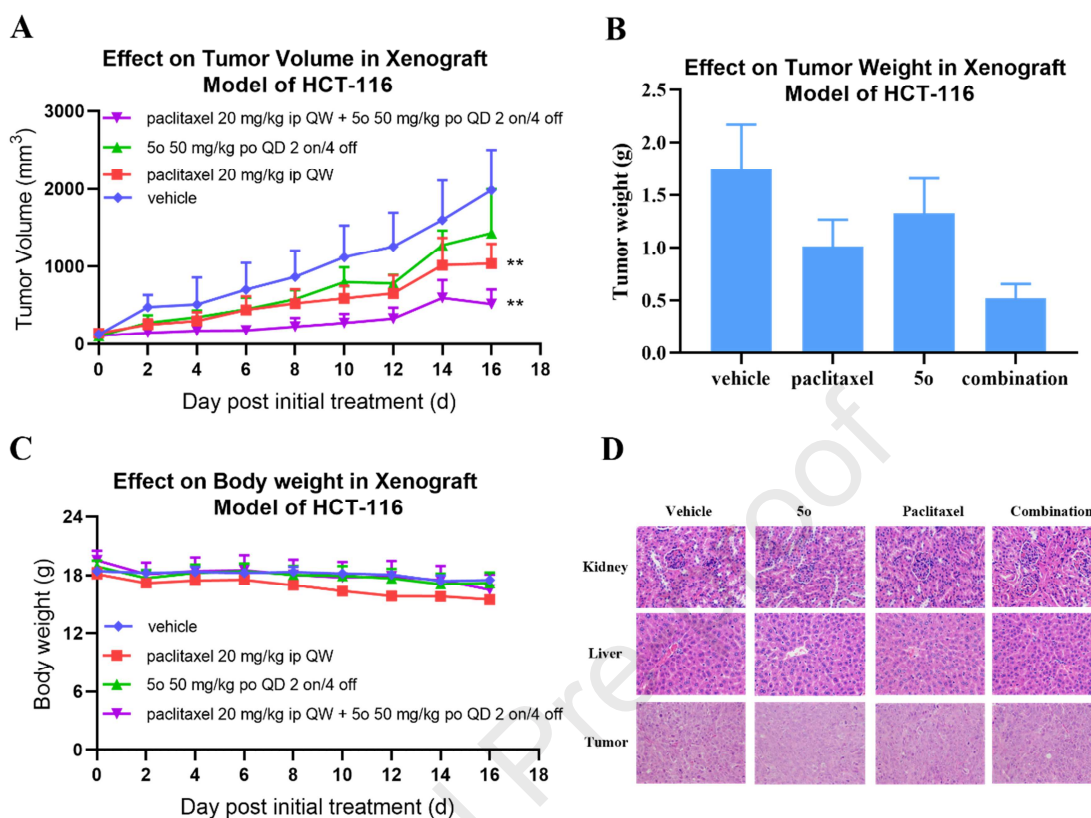


Figure 6. *In vivo* anticancer study of **5o** in combination with paclitaxel against HCT-116 tumor xenografts. CB17-SCID mice (n = 5) bearing HCT116 tumor xenografts were treated with **5o**, paclitaxel, a combination of **5o** and paclitaxel, and vehicle, respectively. *P < 0.05, **P < 0.01 (Student's t-test), compared with vehicle. (A) Tumor volume change in HCT-116 xenograft study; (B) Tumor weight of each treatment group at the end point of treatment; (C) Body weight change in HCT-116 xenograft study; (D) Hematoxylin and eosin (H&E) staining images of the dissected kidney, liver and tumor at the end point of treatment.

CONCLUSIONS

In summary, a series of new pyrido[2, 3-*d*]pyrimidin-7(8*H*)-ones were designed and synthesized as new orally bioavailable selective TTK inhibitors. One of the representative

compounds, **5o**, tightly binds TTK with a K_d value of 0.15 nM and potently suppresses TTK kinase function with an IC_{50} value of 23 nM. Compound **5o** also displays reasonable kinome selectivity against a panel of 403 wild-type kinases at 100 nM. Additionally, compound **5o** exhibits good oral pharmacokinetic properties with a C_{max} value of 1228.70 $\mu\text{g/L}$, a $T_{1/2}$ value of 6.0 hrs, and a bioavailability value of 45.3%, respectively, at an administered dose of 25 mg/kg in SD rats. Further biological investigation demonstrates that compound **5o** potently induces chromosome missegregation and aneuploidy, exhibiting promising anti-proliferative activity in HCT-116 human colorectal cancer cells with an IC_{50} value of 0.41 μM . Combination of **5o** with paclitaxel demonstrated promising *in vivo* efficacy in an HCT-116 xenograft model with a tumor growth inhibition (TGI) value of 78%. Inhibitor **5o** may be utilized as a new research tool for further biological investigation to validate the therapeutic potential of TTK inhibition.

EXPERIMENTAL SECTION

General Methods for Chemistry. All reagents and solvents used were purchased from commercial sources without further purification. Flash chromatography was performed using 300 mesh silica gel. All reactions were monitored by thin-layer chromatography (TLC) using silica gel plates with fluorescence F254 and UV light visualization. ^1H NMR spectra were recorded on a Bruker AV-400 spectrometer at 400 MHz or a Bruker AV-500 spectrometer at 500 MHz. ^{13}C NMR spectra were recorded on a Bruker AV-500 spectrometer at 125 MHz. Coupling constants (J) are expressed in hertz (Hz). Chemical shifts (δ) of NMR are reported in parts per million (ppm) units relative to an internal standard (TMS). High resolution ESI-MS on an Applied Biosystems Q-STAR Elite

ESI-LC-MS/MS mass spectrometer. Purity of all of the final compounds were determined by reverse phase high performance liquid chromatography (HPLC) analysis to be >95%. HPLC instrument: Dionex Summit HPLC (column, Diamonsil C18, 5.0 μm , 4.6 mm \times 250 mm (Dikma Technologies); detector, PDA-100 photodiode array; injector, ASI-100 autoinjector; pump, p-680A). A flow rate of 1.0 mL/min was used with mobile phase of MeOH in H₂O with 0.1% modifier (ammonia, v/v).

General Procedure for the Preparation of Compounds 5e-5g, 5v and 5w.

Ethyl 4-(((1S,4S)-4-((tert-butoxycarbonyl)amino)cyclohexyl)amino)-2-(methylthio)pyrimidine-5-carboxylate (7v). To a suspension of ethyl 4-chloro-2-(methylthio)pyrimidine-5-carboxylate (31.4 g, 135 mmol) and K₂CO₃ (37.3 g, 270 mmol) in MeCN (200 ml), *tert*-butyl((1S, 4S)-4-aminocyclohexyl)carbamate (32.2 g, 150 mmol) was added in batches within 30 minutes. The mixture was stirred at room temperature overnight. After the reaction was completed as monitored by TLC, the solution was concentrated by rotary evaporation, and the residue was diluted with ethyl acetate (EA) and water. The aqueous layer was re-extracted with EA for 3 times. The combined organic layers were washed with water and brine, dried over Na₂SO₄, and concentrated *in vacuo*. The residue was purified by flashing column chromatography (SiO₂, 10-20% EA in petroleum ether) to give **7v** (white solid, 42.2 g, yield 76%). ¹H NMR (400 MHz, CDCl₃) δ 8.62 (s, 1 H), 8.46 (d, J = 6.1 Hz, 1 H), 4.55 (s, 1 H), 4.32 (m, 3 H), 3.62 (s, 1H), 2.51 (s, 3 H), 1.87-1.77 (m, 6 H), 1.53 (m, 2 H), 1.45 (s, 9 H), 1.37 (t, J = 7.0 Hz, 3 H). MS (ESI) m/z 411.2 [M+H]⁺.

***tert*-Butyl((1*S*,4*S*)-4-((5-(hydroxymethyl)-2-(methylthio)pyrimidin-4-yl)amino)cyclohexyl)carbamate (**8v**)**. A suspension of LiAlH₄ (14.0 g, 368.3 mmol) in anhydrous THF (100 mL) was added dropwise to a solution of **7v** (75.5 g, 184.1 mmol) in anhydrous THF (300 mL) under stirring for 1 hr at -40 °C. The mixture was then slowly warmed to 0 °C, and stirred for another 2 hrs. 14 mL H₂O was added dropwise to quench the reaction, and further 14 mL 15% aqueous NaOH and 14 mL H₂O was added consequently. The mixture was stirred at room temperature for 10 minutes and was diluted with EA and DCM, filtered through celite. The combined organic layers were dried over Na₂SO₄, and concentrated *in vacuo*. The residue was purified by flashing column chromatography (SiO₂, 2.5- 5% MeOH in DCM) to give **8v** (white solid, 37.2 g, yield 55%). ¹H NMR (400 MHz, CDCl₃) δ 7.54 (s, 1 H), 6.17 (d, *J* = 6.8 Hz, 1 H), 4.66 (s, 1 H), 4.46 (s, 2 H), 4.18 (s, 1 H), 3.58 (s, 1 H), 2.45 (s, 3 H), 1.75 (m, 6 H), 1.49 (m, 2 H), 1.42 (s, 9 H). MS (ESI) *m/z* 369.1 [M+H]⁺.

***tert*-Butyl((1*S*,4*S*)-4-((5-formyl-2-(methylthio)pyrimidin-4-yl)amino)cyclohexyl)carbamate (**9v**)**. MnO₂ (40.0 g, 46.2 mmol) was added to a solution of **8v** (17.0 g, 46.2 mmol) in DCM (200 ml) in three times within 1.5 hrs. The mixture was stirred at room temperature overnight, and filtered through celite. The organic layer was concentrated *in vacuo*, and the residue was purified by flashing column chromatography (SiO₂, 2.5 - 5% MeOH in DCM) to give **9v** (white solid, 15.7 g, yield 93%). ¹H NMR (400 MHz, CDCl₃) δ 9.69 (s, 1 H), 8.79 (d, *J* = 6.4 Hz, 1 H), 4.59 (s, 1 H), 4.34 (s, 1 H), 3.63 (s, 1 H), 2.52 (s, 3 H), 1.83 (m, 6 H), 1.56 (m, 2 H), 1.44 (s, 9 H). MS (ESI) *m/z* 367.2 [M+H]⁺.

***tert*-Butyl((1*S*,4*S*)-4-((5-(cyclopropyl(hydroxy)methyl)-2-(methylthio)pyrimidin-4-yl)amino)cyclohexyl)carbamate (10v).** Cyclopropylmagnesium bromide in THF (1 N, 25.8 mL, 25.8 mmol) was added dropwise to a solution of **9v** (4.7 g, 12.9 mmol) in anhydrous THF (25 mL) at -78 °C. The mixture was then slowly warmed to -40 °C, and stirred for another 2 hrs. The reaction was quenched with aqueous NH₄Cl and extracted with DCM. The combine organic layers were dried over Na₂SO₄, and concentrated *in vacuo*. The residue was purified by flashing column chromatography (SiO₂, 2.5- 5% MeOH in DCM) to give **10v** (white solid, 3.3 g, yield 63%). ¹H NMR (400 MHz, CDCl₃) δ 7.80 (s, 1 H), 6.48 (d, *J* = 6.6 Hz, 1 H), 4.54 (s, 1 H), 4.22 (s, 1 H), 3.77 (d, *J* = 8.6 Hz, 1 H), 3.60 (s, 1H), 2.60 (br, 1 H), 2.48 (s, 3 H), 1.78 (m, 6 H), 1.50 (m, 2 H), 1.45(s, 9 H), 1.34 (m, 1 H), 0.71 (m, 1 H), 0.63 (m, 1 H), 0.46 (m, 1 H), 0.27 (m, 1 H). MS (ESI) *m/z* 409.7 [M+H]⁺.

***tert*-Butyl((1*S*,4*S*)-4-((5-(cyclopropanecarbonyl)-2-(methylthio)pyrimidin-4-yl)amino)cyclohexyl)carbamate (11v).** MnO₂ (3.80 g, 43.7 mmol) was added to a solution of **10v** (1.78g, 4.4 mmol) in DCM (20 ml) in three times within 1.5 hrs. The mixture was stirred at room temperature overnight, and filter through celite. The organic layer was concentrated *in vacuo*, and the residue was purified by flash column chromatography (SiO₂, 2.5 - 5% MeOH in DCM) to give **11v** (white solid, 1.42 g, yield 80%). ¹H NMR (400 MHz, CDCl₃) δ 9.52 (d, *J* = 7.0 Hz, 1H), 8.79 (s, 1 H), 4.56 (s, 1 H), 4.33 (m, 1 H), 3.60 (s, 1 H), 2.52 (br, 4 H), 1.84 (m, 2 H), 1.77 (m, 4 H), 1.51 (m, 2 H), 1.44 (s, 9 H), 1.18 (m, 2 H), 1.00 (m, 2 H). MS (ESI) *m/z* 407.5 [M+H]⁺.

tert*-Butyl((1*S*,4*S*)-4-(5-cyclopropyl-2-(methylthio)-7-oxopyrido[2,3-*d*]pyrimidin-8(7*H*)-yl)cyclohexyl)carbamate (12*v*)**. To a round-bottom flask equipped with a condenser was added **11*v (1.7 g, 4.2 mmol), (2-Methoxy-2-oxoethylidene) triphenylphosphorane (2.8 g, 8.4 mmol) and anhydrous toluene (25 ml). The mixture was refluxed under argon and stirred for 48 hrs. The mixture was concentrated *in vacuo*. The residue was purified by flashing column chromatography (SiO₂, 1 - 5% MeOH in DCM) to give **12*v*** (white solid, 326 mg, yield 18%). ¹H NMR (400 MHz, CDCl₃) δ 9.04 (s, 1 H), 6.23 (s, 1 H), 5.44 (s, 1 H), 5.10 (s, 1 H), 3.96 (s, 1 H), 2.79 (d, *J* = 9.8 Hz, 2 H), 2.66 (s, 3 H), 1.95 (d, *J* = 14.5 Hz, 2 H), 1.48 (s, 9 H), 1.11 (m, 2 H), 0.80 (m, 2 H). MS (ESI) *m/z* 453.3 [M+Na]⁺.

tert*-Butyl ((1*S*,4*S*)-4-(5-cyclopropyl-2-(methylsulfonyl)-7-oxopyrido[2,3-*d*]pyrimidin-8(7*H*)-yl)cyclohexyl)carbamate (13*v*)**. To a cool (0 °C) solution of **12*v (326 mg, 0.8 mmol) was added *m*-CPBA (392 mg, 2.3 mmol). The mixture was stirred at 0 °C for 3 hrs. The reaction was quenched with aqueous sodium thiosulfate (5 ml) and extracted with DCM. The combine organic layers were dried with Na₂SO₄, and concentrated *in vacuo*. The residue was purified by flashing column chromatography (SiO₂, 1 - 5% MeOH in DCM) to give **13*v*** (white solid, 338 mg, yield 96%). ¹H NMR (400 MHz, CDCl₃) δ 9.35 (s, 1 H), 6.52 (s, 1 H), 5.52 (s, 1 H), 5.34 (s, 1 H), 4.02 (s, 1 H), 3.38 (s, 3 H), 2.90 (br, 2 H), 2.10 (m, 1H), 1.96 (d, *J* = 11.9 Hz, 2 H), 1.70 (m, 2 H), 1.56 (d, *J* = 11.4 Hz, 2 H), 1.49 (s, 9 H), 1.20 (m, 2 H), 0.87 (m, 2 H). MS (ESI) *m/z* 485.4 [M+Na]⁺.

8-((1*S*,4*S*)-4-aminocyclohexyl)-5-cyclopropyl-2-((2-methoxy-4-(4-methylpiperazin-1-yl)phenyl)amino)pyrido[2,3-*d*]pyrimidin-7(8*H*)-one (14*v*). To a solution of **13*v*** (338

mg, 0.7 mmol) and 2-methoxy-4-(4-methylpiperazin-1-yl) aniline (177.9 mg, 0.8 mmol) in anhydrous 2-BuOH (5 ml) was added TFA (65 μ l, 0.9 mmol). The mixture was stirred at 95 °C under argon for 18 hrs. The volatiles were removed by rotary evaporation and TFA (2ml), DCM (4ml) was added. The mixture was stirred at room temperature for 2 hrs. After the reaction was completed, as monitored by TLC, the volatiles were removed *in vacuo*, and the residue was diluted with DCM and neutralize with aqueous NaHCO₃, and was extracted with DCM. The combined organic layers were dried with Na₂SO₄, and concentrated *in vacuo*. The residue was purified by flashing column chromatography (SiO₂, 1 - 10% MeOH in DCM) to give **14v** (yellow solid, 76 mg, yield 21%). ¹H NMR (400 MHz, CDCl₃) δ 8.93 (s, 1 H), 8.14 (s, 1 H), 7.61 (s, 1 H), 6.58-6.54 (m, 2 H), 6.02 (s, 1 H), 5.42 (m, 1 H), 3.91 (s, 3 H), 3.26 (s, 1 H), 3.21 (m, 4 H), 2.89 (q, *J* = 13.3 Hz, 2 H), 2.61 (m, 4 H), 2.37 (s, 3 H), 1.85 (d, *J* = 12.3 Hz, 2 H), 1.73 (t, *J* = 13.3 Hz, 2 H), 1.50 (d, *J* = 12.2 Hz, 2 H), 1.07 (d, *J* = 7.8 Hz, 2 H), 0.85 (t, *J* = 8.9 Hz, 1 H), 0.79 (d, *J* = 4.9 Hz, 2 H). MS (ESI) *m/z* 504.9 [M+H]⁺.

***N*-((1*S*,4*S*)-4-(5-cyclopropyl-2-((2-methoxy-4-(4-methylpiperazin-1-yl)phenyl)amino)-7-oxopyrido[2,3-*d*]pyrimidin-8(7*H*)-yl)cyclohexyl)propionamide (5v)**. Propionyl chloride (14.5 μ l, 0.2 mmol) in 10 ml anhydrous DCM was added dropwise to a cool (0 °C) solution of **14v** (76 mg, 0.2 mmol) and DIEA (31.6 μ l, 0.2 mmol) in 10 ml anhydrous DCM. The mixture was stirred at 0 °C for 10 minutes until the reaction was completed. The reaction mixture was washed with 1N aqueous HCl, and extracted with DCM. The combined organic layers were dried with Na₂SO₄, and concentrated *in vacuo*. The residue was purified by flashing column chromatography (SiO₂, 1 - 10% MeOH in

DCM) to give **5v** (yellow solid, 70 mg, yield 83%). ¹H NMR (400 MHz, CDCl₃), δ 8.95 (s, 1 H), 8.19 (d, *J* = 8.6 Hz, 1 H), 7.67 (s, 1 H), 6.57-6.54 (m, 2 H), 6.24 (s, 1 H), 6.00 (s, 1 H), 5.54 (t, *J* = 11.8 Hz, 1H), 4.35 (br, 1 H), 3.91 (s, 3 H), 3.23 (t, *J* = 4.7 Hz, 3 H), 2.73 (q, *J* = 9.9 Hz, 4 H), 2.65 (t, *J* = 4.7 Hz, 4 H), 2.40 (s, 3 H), 2.30 (q, *J* = 7.6 Hz, 3 H), 2.03 (m, 1 H), 1.94 (d, *J* = 13.4Hz, 2 H), 1.69 (d, 2 H, *J* = 13.7 Hz), 1.61 (d, *J* = 15.7 Hz, 2 H), 1.24 (d, *J* = 6.8 Hz, 2 H), 1.20 (d, *J* = 7.6 Hz, 2 H), 1.10-1.05 (m, 2 H), 0.81-0.77(m, 2 H). ¹³C NMR (125 MHz, CDCl₃), δ 173.5, 164.7, 158.9, 156.2, 155.6, 150.4, 149.7, 148.0, 121.3, 120.2, 114.3, 107.9, 107.8, 100.3, 55.8, 55.1, 49.8, 46.0, 42.7, 30.1, 22.3, 10.8, 10.2, 7.4. HRMS (ESI) for C₃₁H₄₁N₇O₃ [M+H]⁺, Calcd: 561.3323, Found: 561.3346. HPLC analysis: MeOH-H₂O (90: 10), RT= 16.28 min, 99.5% purity.

General Procedure for the Preparation of Compounds 5b-5d; 5h-5u and 5x-5z.

tert-Butyl((1*S*,4*S*)-4-((5-bromo-2-chloropyrimidin-4-yl)amino)cyclohexyl)carbamate (**16h**). Compound **16h** was prepared following a similar procedure to that used for preparation of **7v**. White solid, yield 96%. ¹H NMR (400 MHz, CDCl₃), δ 8.11 (s, 1 H), 5.48 (d, *J* = 7.2 Hz, 1 H), 4.59 (s, 1 H), 4.17-4.13 (m, 1 H), 3.67 (s, 1 H), 1.88-1.79 (m, 4 H), 1.69-1.57 (m, 4 H), 1.44 (s, 9 H), 1.33-1.28 (m, 1 H). MS (ESI) *m/z* 406.4 [M+H]⁺.

tert-Butyl((1*S*,4*S*)-4-(2-chloro-5-methyl-7-oxopyrido[2,3-*d*]pyrimidin-8(7*H*)-yl)cyclohexyl)carbamate (**18h**). To a round-bottom flask equipped with a condenser was add **16h** (25.6 g, 63.1 mmol), crotonic acid (**17h**) (27.1 g, 315.3 mmol), bis (benzonitrile) palladium (II) dichloride (1.2 g, 3.2 mmol), tri-*o*-tolylphosphine (958 mg, 3.2 mmol), DIEA (109 ml, 630 mmol) and anhydrous THF (200 ml). The mixture was reflux for 16 hrs under argon. Ac₂O (16 ml, 16.9 mmol) was added and the mixture were heated to

95 °C and stirred for another 24 hrs. After the reaction mixture was cooled to room temperature, filtered through celite. The volatiles were removed by rotary evaporation, and the residue was diluted with DCM and water. The aqueous layer was re-extracted with DCM. The combined organic layers were washed with H₂O and brine, dried with Na₂SO₄, and concentrated *in vacuo*. The residue was purified by flashing column chromatography (SiO₂, 20- 50% EA in petroleum ether) to give **18h** (white solid ,7.8 g, yield 32%). ¹H NMR (400 MHz, CDCl₃) δ 8.76 (s, 1 H), 6.55 (s, 1 H), 5.38-5.25 (m, 2 H), 4.00 (d, *J* = 2.8 Hz, 1 H), 2.79 (d, *J* = 10.8 Hz, 2 H), 2.45 (s, 3 H), 1.95-1.91 (m, 2 H), 1.91-1.65 (m, 2 H), 1.57-1.54 (m, 2 H), 1.47 (s, 9 H) MS (ESI) *m/z* 393.6 [M+Na]⁺.

8-((1S,4S)-4-aminocyclohexyl)-2-((2-methoxy-4-(4-methylpiperazin-1-yl)phenyl)amino)-5-methylpyrido[2,3-*d*]pyrimidin-7(8*H*)-one (19h). To a solution of **18h** (1.6 g, 4 mmol) and 2-methoxy-4-(4-methylpiperazin-1-yl) aniline (929.7 mg, 4.4 mmol) in anhydrous 2-BuOH (8 ml) was added TFA (0.4 ml, 4.8 mmol). The mixture was stirred at 95 °C under argon for 18 hrs. The volatiles were removed by rotary evaporation and TFA (3 ml), DCM (3 ml) was added. The mixture was stirred at room temperature for 2 hrs. After the reaction was completed, as monitored by TLC, the volatiles were removed *in vacuo*, and the residue was diluted with DCM and neutralized with aqueous NaHCO₃ before being extracted with DCM. The combine organic layers were dried with Na₂SO₄, and concentrated *in vacuo*. The residue was purified by flashing column chromatography (SiO₂, 1 - 10% MeOH in DCM) to give **19h** (yellow solid, 1.3 g, yield 68%). ¹H NMR (400 MHz, CDCl₃) δ 8.59 (s, 1H), 8.14 (s, 1 H), 7.63 (s, 1 H), 6.57-6.53 (m, 2 H), 6.20 (s, 1 H), 5.42 (br, 1 H), 3.89 (s, 3 H), 3.20 (m, 4 H), 2.90 (q, *J* = 12.6 Hz, 2

H), 2.60 (m, 4 H), 2.16 (s, 3 H), 1.81 (d, $J = 12.6$ Hz, 2 H), 1.71 (t, $J = 13.5$ Hz, 2 H), 1.48 (d, $J = 11.3$ Hz, 2 H), 1.23 (m, 2 H). MS (ESI) m/z 478.3 $[M+H]^+$.

N*-((1*S*,4*S*)-4-(2-((2-methoxy-4-(4-methylpiperazin-1-yl)phenyl)amino)-5-methyl-7-oxopyrido[2,3-*d*]pyrimidin-8(7*H*)-yl)cyclohexyl)propionamide (5*h*)**. Compound **5*h was prepared from **19*h*** following a similar procedure to that used for preparation of **5*v***. Yellow solid, yield 58%. ^1H NMR (400 MHz, CDCl_3), δ 8.62 (s, 1 H), 8.18 (d, $J = 8.7$ Hz, 1 H), 7.68 (s, 1 H), 6.57-6.53 (m, 2 H), 6.26 (s, 1 H), 6.19 (s, 1 H), 5.55 (m, 1 H), 4.34 (m, 1 H), 3.91 (s, 3 H), 3.21 (t, 4 H, $J = 5.0$ Hz), 2.79-2.69 (m, 2 H), 2.61 (t, $J = 4.8$ Hz, 4 H), 2.37 (s, 6 H), 2.32-2.27 (q, $J = 7.6$ Hz, 2 H), 1.95 (d, $J = 13.1$ Hz, 2 H), 1.71-1.68 (m, 2 H), 1.63-1.59 (m, 3 H), 1.21 (t, $J = 7.6$ Hz, 3 H). ^{13}C NMR (125 MHz, CDCl_3), δ 173.5, 164.1, 158.8, 155.9, 155.6, 149.6, 148.1, 144.9, 121.0, 120.2, 118.7, 107.7, 107.4, 100.1, 55.7, 55.1, 52.8, 49.8, 46.1, 42.6, 30.1, 29.9, 22.3, 17.1, 10.1. HRMS (ESI) for $\text{C}_{29}\text{H}_{39}\text{N}_7\text{O}_3$ $[M+H]^+$, Calcd: 534.3187, Found: 534.3188, RT= 3.04 min. HPLC analysis: MeOH- H_2O (85: 15), RT= 12.11 min, 96.7% purity.

(S)*-2-((2-methoxy-4-(4-methylpiperazin-1-yl)phenyl)amino)-5-methyl-8-(1-propionylpyrrolidin-3-yl)pyrido[2,3-*d*]pyrimidin-7(8*H*)-one (5*b*)**. Compound **5*b was prepared following a similar procedure to that used for preparation of **5*h***. Yellow solid, yield 89%. ^1H NMR (400 MHz, CDCl_3), δ 8.62 (s, 1 H), 7.99 (m, 1 H), 7.65 (s, 1 H), 7.48 (s, 1 H), 6.54-6.51 (m, 2 H), 6.25-6.13 (m, 2 H), 4.32 (s, 1 H), 4.02 (m, 1 H), 3.90 (s, 3 H), 3.79 (br, 1H), 3.62 (m, 1H), 3.52 (m, 1H), 3.21 (m, 4 H), 3.03-2.85 (m, 1 H), 2.59 (s, 4 H), 2.36 (s, 6 H), 2.24-2.19 (m, 2 H), 2.07-2.05 (m, 1 H), 1.21-1.10 (m, 4 H). ^{13}C NMR (125 MHz, CDCl_3), δ 172.7, 172.4, 163.7, 163.6, 159.3, 159.0, 156.3, 156.2, 156.1, 150.7,

150.1, 148.8, 148.6, 145.4, 145.3, 121.8, 120.9, 120.8, 120.6, 118.1, 117.8, 107.9, 107.8, 107.7, 100.4, 100.1, 55.9, 55.3, 51.0, 49.9, 49.8, 49.6, 46.6, 46.2, 45.9, 44.7, 28.0, 27.5, 25.7, 17.3, 9.2, 9.1. HRMS (ESI) for $C_{27}H_{35}N_7O_3$ $[M+H]^+$, Calcd: 506.28741, Found: 506.2877, RT= 2.94 min. HPLC analysis: MeOH-H₂O (85: 15), RT= 7.31 min, 99.4% purity.

2-((2-methoxy-4-(4-methylpiperazin-1-yl)phenyl)amino)-5-methyl-8-(1-propionylzetidin-3-yl)pyrido[2,3-*d*]pyrimidin-7(8*H*)-one (5c). Compound **5c** was prepared following a similar procedure to that used for preparation of **5h**. Yellow solid, yield 88%. ¹H NMR (400 MHz, CDCl₃), δ 8.36 (s, 1 H), 7.41 (d, $J = 5.0$ Hz, 1 H.), 6.92 (d, $J = 8.4$ Hz, 1 H), 6.55 (d, $J = 2.4$ Hz, 1 H), 6.50 (dd, $J = 2.4, 2.4$ Hz, 1 H), 5.89 (s, 1 H), 4.93-4.88 (m, 1 H), 4.56 (dd, $J = 10.2, 10.2$ Hz, 1 H), 4.21-4.12 (m, 2 H), 3.79 (s, 3 H), 3.53-3.48 (m, 1 H), 3.17 (t, $J = 4.9$ Hz, 4 H), 2.58 (t, $J = 4.8$ Hz, 4 H), 2.35 (s, 3 H), 2.31 (s, 3 H), 2.28-2.23 (q, 2 H), 1.16 (t, $J = 7.6$ Hz, 3 H). ¹³C NMR (125 MHz, CDCl₃), δ 174.9, 161.5, 156.9, 152.5, 151.6, 148.9, 148.5, 146.8, 130.3, 123.6, 112.8, 108.9, 102.2, 97.6, 58.7, 56.1, 55.6, 50.4, 50.2, 46.5, 42.8, 30.1, 30.0, 17.6, 10.1. HRMS (ESI) for $C_{26}H_{33}N_7O_3$ $[M+H]^+$, Calcd: 492.2718, Found: 492.2721, RT= 1.47 min. HPLC analysis: MeOH-H₂O (80: 20), RT= 6.03 min, 98.0% purity.

(R)-2-((2-methoxy-4-(4-methylpiperazin-1-yl)phenyl)amino)-5-methyl-8-(1-propionylpyrrolidin-3-yl)pyrido[2, 3-*d*]pyrimidin-7(8*H*)-one (5d). Compound **5d** was prepared following a similar procedure to that used for preparation of **5h**. Yellow solid, yield 56%. ¹H NMR (400 MHz, CDCl₃), δ 8.62 (s, 1 H), 7.97 (s, 1 H), 7.65-7.49 (m, 1 H), 6.53 (m, 2 H), 6.25-6.15 (m, 2 H), 4.31 (s, 1 H), 3.99-3.97 (m, 1 H), 3.89 (s, 3 H), 3.78 (s,

1 H), 3.61 (t, $J = 8.0$ Hz, 1 H), 3.51(m, 1 H), 3.20 (br, 4 H), 3.03-2.88 (m, 1 H), 2.59 (br, 4 H), 2.35 (s, 6 H), 2.22-2.20 (m, 2 H), 1.24-1.11 (m, 4 H). ^{13}C NMR (125 MHz, CDCl_3), δ 172.6, 172.3, 163.6, 163.5, 159.0, 158.8, 156.2, 156.1, 155.9, 155.8, 149.9, 148.6, 148.4, 145.4, 145.2, 121.5, 120.6, 120.3, 117.9, 117.6, 107.7, 107.6, 100.2, 99.9, 55.7, 55.1, 50.8, 49.7, 49.6, 49.5, 46.5, 46.1, 45.8, 44.5, 27.9, 27.4, 17.2, 9.1, 9.0. HRMS (ESI) for $\text{C}_{27}\text{H}_{35}\text{N}_7\text{O}_3$ $[\text{M}+\text{H}]^+$, Calcd: 506.28741, Found: 506.2877, RT= 2.95 min. HPLC analysis: MeOH- H_2O (75: 25), RT= 11.30 min, 96.2% purity.

(R)-2-((2-methoxy-4-(4-methylpiperazin-1-yl)phenyl)amino)-5-methyl-8-(1-propionylpiperidin-3-yl)pyrido[2,3-d]pyrimidin-7(8H)-one (5e). Compound **5e** was prepared following a similar procedure to that used for preparation of **5v**. Yellow solid, yield 52%. ^1H NMR (400 MHz, CDCl_3), δ 8.60 (d, $J = 9.6$ Hz, 1 H), 8.09 (s, 1 H), 7.64 (s, 1 H), 6.55-6.51 (m, 2 H), 6.21 (s, 1 H), 5.42 (s, 1 H), 4.66 (s, 1 H), 4.23 (m, 1 H), 3.89 (s, 4 H), 3.71 (s, 1 H), 3.20 (br, 4 H), 2.85 (m, 1 H), 2.60 (s, 4 H), 2.36 (s, 6 H), 2.28 (m, 2 H), 1.89-1.79 (m, 2 H), 1.20-1.07 (m, 3 H). ^{13}C NMR (125 MHz, $\text{DMSO}-d_6$), δ 171.1, 170.9, 156.8, 155.3, 145.9, 118.7, 106.4, 106.1, 99.7, 55.3, 54.6, 48.3, 46.5, 45.7, 25.9, 25.6, 25.1, 16.6, 9.5, 9.4. HRMS (ESI) for $\text{C}_{28}\text{H}_{37}\text{N}_7\text{O}_3$ $[\text{M}+\text{H}]^+$, Calcd: 520.3031, Found: 520.3031, RT= 2.97 min. HPLC analysis: MeOH- H_2O (80: 20), RT= 8.31 min, 99.3% purity.

(S)-2-((2-methoxy-4-(4-methylpiperazin-1-yl)phenyl)amino)-5-methyl-8-(1-propionylpiperidin-3-yl)pyrido[2,3-d]pyrimidin-7(8H)-one (5f). Compound **5f** was prepared following a similar procedure to that used for preparation of **5v**. Yellow solid, yield 55%. ^1H NMR (400 MHz, CDCl_3), δ 8.55 (d, $J = 12$ Hz, 1 H), 8.03 (s, 1 H), 7.65 (s, 1 H),

6.50-6.42 (m, 2 H), 6.14 (d, $J = 11.9$ Hz, 1 H), 5.39 (s, 1 H), 4.61 (s, 1 H), 4.19 (t, $J = 11.7$ Hz, 1 H), 3.84 (s, 3 H), 3.65 (s, 1 H), 3.18-3.12 (m, 4 H), 2.85-2.76 (m, 1 H), 2.56 (m, 4 H), 2.32 (s, 6 H), 2.29-2.22 (m, 2 H), 1.75 (br, 2 H), 1.59-1.55 (m, 1 H), 1.15 (s, 1 H), 1.02 (s, 2 H). ^{13}C NMR (125 MHz, CDCl_3), δ 172.6, 172.1, 164.0, 159.4, 156.2, 156.0, 145.2, 145.0, 118.4, 107.9, 107.6, 100.6, 100.3, 55.9, 55.3, 50.1, 49.8, 47.4, 46.3, 43.3, 42.2, 26.9, 26.7, 25.8, 17.3, 9.9, 9.7. HRMS (ESI) for $\text{C}_{28}\text{H}_{37}\text{N}_7\text{O}_3$ $[\text{M}+\text{H}]^+$, Calcd: 520.3031, Found: 520.3036, RT= 2.97 min. HPLC analysis: MeOH- H_2O (85 :15), RT= 7.26 min, 99.9% purity.

2-((2-methoxy-4-(4-methylpiperazin-1-yl)phenyl)amino)-5-methyl-8-(1-propionylpiperidin-4-yl)pyrido[2,3-*d*]pyrimidin-7(8*H*)-one (5g). Compound **5g** was prepared following a similar procedure to that used for preparation of **5v**. Yellow solid, yield 62%. ^1H NMR (400 MHz, CDCl_3), δ 8.60 (s, 1 H), 8.14 (d, $J = 8.6$ Hz, 1 H), 7.65 (s, 1 H), 6.56-6.52 (m, 2 H), 6.22 (s, 1 H), 5.63 (br, 1 H), 4.89 (d, $J = 13.0$ Hz, 1 H), 4.02 (d, $J = 12.4$ Hz, 1 H), 3.91 (s, 3 H), 3.21 (t, $J = 5.0$ Hz, 4 H), 3.13 (t, $J = 12.9$ Hz, 1 H), 2.99-2.97 (m, 1 H), 2.86 (br, 1 H), 2.68 (t, $J = 11.5$ Hz, 1 H), 2.60 (t, $J = 4.8$ Hz, 4 H), 2.44-2.39 (q, 2 H), 2.36 (s, 6 H), 1.72-1.69 (m, 2 H), 1.19 (t, $J = 7.4$ Hz, 3 H). ^{13}C NMR (125 MHz, CDCl_3), δ 172.3, 163.7, 158.7, 155.9, 149.6, 148.1, 144.8, 120.9, 120.2, 118.4, 107.7, 100.0, 55.7, 55.1, 49.7, 46.1, 45.8, 42.1, 29.7, 28.3, 27.6, 26.6, 17.1, 9.6. HRMS (ESI) for $\text{C}_{28}\text{H}_{37}\text{N}_7\text{O}_3$ $[\text{M}+\text{H}]^+$, Calcd: 520.3031, Found: 520.3029, RT= 2.98 min. HPLC analysis: MeOH- H_2O (75: 25), RT= 13.09 min, 96.0% purity.

***N*-((1*R*,4*R*)-4-(2-((2-methoxy-4-(4-methylpiperazin-1-yl)phenyl)amino)-5-methyl-7-oxopyrido[2,3-*d*]pyrimidin-8(7*H*)-yl)cyclohexyl)propionamide (5i).** Compound **5i**

was prepared following a similar procedure to that used for preparation of **5h**. Yellow solid, yield 63%. ^1H NMR (400 MHz, CDCl_3), δ 8.58 (s, 1 H), 8.10 (s, 1 H), 7.50 (br, 1 H), 6.58 (d, $J = 2.2$ Hz, 1 H), 6.22 (s, 1 H), 5.30 (d, $J = 7.6$ Hz, 2 H), 3.96-3.95 (m, 1 H), 3.91 (s, 3 H), 3.24 (br, 4 H), 2.92 (br, 2 H), 2.59 (t, $J = 4.6$ Hz, 4 H), 2.36 (s, 3 H), 2.35 (s, 3 H), 2.20 (q, $J = 7.6$ Hz, 2 H), 2.12-2.11 (m, 2 H), 1.66 (d, 2 H, $J = 11.2$ Hz), 1.37-1.25 (m, 4 H), 1.16 (t, $J = 7.6$ Hz, 3 H). ^{13}C NMR (125 MHz, CDCl_3), δ 172.8, 163.8, 159.2, 156.3, 155.8, 150.5, 148.7, 144.7, 122.0, 120.7, 118.1, 108.3, 107.6, 100.2, 55.8, 55.3, 53.0, 49.7, 47.7, 46.1, 33.1, 29.9, 27.0, 22.7, 17.1, 14.1, 9.9. HRMS (ESI) for $\text{C}_{29}\text{H}_{39}\text{N}_7\text{O}_3$ $[\text{M}+\text{H}]^+$, Calcd: 534.3187, Found: 534.3184, RT= 3.05 min. HPLC analysis: MeOH- H_2O (85: 15), RT= 9.15 min, 99.9% purity.

***N*-((1*S*,4*S*)-4-(5-methyl-2-((2-methyl-4-(4-methylpiperazin-1-yl)phenyl)amino)-7-oxopyrido[2,3-*d*]pyrimidin-8(7*H*)-yl)cyclohexyl)propionamide (5ha)**. Compound **5ha** was prepared following a similar procedure to that used for preparation of **5h**. Yellow solid, yield 58%. ^1H NMR (400 MHz, CDCl_3), δ 8.59 (s, 1 H), 7.58 (d, $J = 7.6$ Hz, 1 H), 6.93 (s, 1 H), 6.82-6.79 (m, 2 H), 6.27 (br, 1 H), 6.17 (s, 1 H), 5.42 (m, 1 H), 4.27 (m, 1 H), 3.20 (m, 4 H), 2.71 (q, $J = 12.0$ Hz, 2 H), 2.60 (m, 4 H), 2.36 (s, 6 H), 2.30 (s, 3 H), 2.28-2.24 (m, 2 H), 1.88 (d, $J = 13.2$ Hz, 2 H), 1.59-1.51 (m, 4 H), 1.19 (t, $J = 7.6$ Hz, 3 H). ^{13}C NMR (125 MHz, CDCl_3), δ 173.4, 164.2, 160.2, 156.3, 155.8, 149.1, 144.9, 128.9, 125.0, 118.9, 118.2, 114.2, 107.6, 55.2, 52.2, 49.2, 46.2, 42.7, 30.2, 29.9, 22.3, 18.7, 17.2, 10.2. HRMS (ESI) for $\text{C}_{29}\text{H}_{39}\text{N}_7\text{O}_2$ $[\text{M}+\text{H}]^+$, Calcd: 518.3238, Found: 518.3237, RT= 1.18 min. HPLC analysis: MeOH- H_2O (90: 10), RT= 11.29 min, 95.8% purity.

***N*-((1*S*,4*S*)-4-(2-((3-methoxy-4-(4-methylpiperazin-1-yl)phenyl)amino)-5-methyl-7-oxopyrido[2,3-*d*]pyrimidin-8(7*H*)-yl)cyclohexyl)propionamide (5hb)**. Compound **5hb** was prepared following a similar procedure to that used for preparation of **5h**. Yellow solid, yield 65%. ^1H NMR (400 MHz, CDCl_3), δ 8.64 (s, 1 H), 7.29 (s, 1 H), 7.20 (d, $J = 7.4$ Hz, 1 H), 7.07 (s, 1H), 6.93 (d, $J = 8.5$ Hz, 1 H), 6.27 (br, 1 H), 6.21 (s, 1 H),

5.51 (m 1 H), 4.32 (m, 1 H), 3.88 (s, 3 H), 3.09(br, 4 H), 2.72 (q, $J = 12.9$ Hz, 2 H), 2.64 (br, 4 H), 2.38 (s, 3 H), 2.36 (s, 3 H), 2.29 (q, $J = 7.5$ Hz, 2 H), 1.93 (m, 2 H), 1.65-1.56 (m, 4 H), 1.21 (t, $J = 7.6$ Hz, 3 H). ^{13}C NMR (125 MHz, CDCl_3), δ 173.3, 164.1, 159.2, 156.0, 155.7, 152.6, 144.7, 137.9, 133.9, 119.1, 118.3, 112.9, 107.8, 105.3, 55.7, 55.3, 52.0, 50.8, 46.2, 42.5, 30.1, 29.7, 21.9, 17.2, 10.1. HRMS (ESI) for $\text{C}_{29}\text{H}_{39}\text{N}_7\text{O}_3$ $[\text{M}+\text{H}]^+$, Calcd: 534.3187, Found: 534.3184, RT= 1.17 min. HPLC analysis: MeOH- H_2O (90: 10), RT= 8.43 min, 99.2% purity.

***N*-((1*S*,4*S*)-4-(5-methyl-2-((3-methyl-4-(4-methylpiperazin-1-yl)phenyl)amino)-7-oxopyrido[2,3-*d*]pyrimidin-8(7*H*)-yl)cyclohexyl)propionamide (5*hc*)**. Compound **5hc** was prepared following a similar procedure to that used for preparation of **5h**. Yellow solid, yield 49%. ^1H NMR (400 MHz, CDCl_3), δ 8.62 (s, 1 H), 7.58 (s, 1 H), 7.49 (s, 1 H), 7.31 (d, $J = 7.8$ Hz, 2 H), 7.02 (d, $J = 8.5$ Hz, 2 H), 6.29 (br, 1 H), 6.20 (s, 1 H), 5.53 (m 1 H), 4.31 (br, 1 H), 2.93 (br, 4 H), 2.73 (q, $J = 13.2$ Hz, 2 H), 2.59 (br, 4 H), 2.36 (s, 6 H), 2.33 (s, 3 H), 2.28 (m, 2 H), 1.92 (d, $J = 12.6$ Hz, 2 H), 1.67-1.57 (m, 4 H), 1.19 (t, $J = 7.4$ Hz, 3 H). ^{13}C NMR (125 MHz, CDCl_3), δ 173.4, 163.9, 158.9, 155.8, 155.5, 147.5, 144.6, 133.8, 133.2, 122.7, 119.2, 118.8, 118.3, 107.4, 55.4, 52.2, 51.7, 46.0, 42.4, 29.8, 29.7, 21.9, 18.0, 17.0, 9.9. HRMS (ESI) for $\text{C}_{29}\text{H}_{39}\text{N}_7\text{O}_2$ $[\text{M}+\text{H}]^+$, Calcd: 518.3238, Found: 518.3234, RT= 1.16 min. HPLC analysis: MeOH- H_2O (90: 10), RT= 10.73 min, 100% purity.

***N*-((1*S*,4*S*)-4-(2-((2-methoxy-4-(4-methylpiperazin-1-yl)phenyl)amino)-5-methyl-7-oxopyrido[2,3-*d*]pyrimidin-8(7*H*)-yl)cyclohexyl)acetamide (5*j*)**. Compound **5j** was prepared following a similar procedure to that used for preparation of **5h**. Yellow solid, yield 56%. ^1H NMR (400 MHz, CDCl_3), δ 8.62 (s, 1 H), 8.18 (d, $J = 8.7$ Hz, 1 H), 7.68 (s, 1 H), 6.57 (d, $J = 2.4$ Hz, 1 H), 6.54 (dd, $J = 2.4, 2.4$ Hz, 1 H), 6.31 (s, 1 H), 6.19 (s, 1 H), 5.58-5.52 (m, 1 H), 4.34-4.32 (m, 1 H), 3.92 (s, 3 H), 3.21 (t, $J = 5.1$ Hz, 4 H), 2.79-2.69 (m, 2 H), 2.62 (t, $J = 4.9$ Hz, 4 H), 2.38 (s, 3 H), 2.37 (s, 3 H), 2.06 (s, 3 H), 1.95 (d, $J = 13.5$ Hz 2 H), 1.71-1.67 (m, 2 H), 1.60 (s, 2 H). ^{13}C NMR (125 MHz, CDCl_3), δ 169.7,

164.3, 159.1, 156.1, 155.9, 149.9, 148.3, 144.9, 121.3, 120.5, 118.9, 107.9, 107.6, 100.4, 55.9, 55.3, 52.9, 50.0, 46.3, 43.1, 30.2, 23.8, 22.5, 17.2. HRMS (ESI) for $C_{28}H_{37}N_7O_3$ $[M+H]^+$, Calcd: 520.3031, Found: 520.3027, RT= 2.98 min. , HPLC analysis: MeOH-H₂O (90: 10), RT= 9.93 min, 99.7% purity.

***N*-((1*S*,4*S*)-4-(2-((2-methoxy-4-(4-methylpiperazin-1-yl)phenyl)amino)-5-methyl-7-oxopyrido[2,3-*d*]pyrimidin-8(7*H*)-yl)cyclohexyl)cyclopropanecarboxamide (5*k*).**

Compound **5k** was prepared following a similar procedure to that used for preparation of **5h**. Yellow solid, yield 74%. ¹H NMR (400 MHz, CDCl₃), δ 8.61 (s, 1 H), 8.17 (d, J = 7.9 Hz, 1 H), 7.68 (br, 1 H), 6.55-6.52 (m, 2 H), 6.18 (s, 1 H), 5.54 (br, 1 H), 4.35 (s, 1 H), 3.90(s, 3 H), 3.20 (br, 4 H), 2.78 (q, J = 12.4 Hz, 4 H), 2.60 (br, 4 H), 2.36 (s, 6 H), 2.25 (s, 2 H), 1.94 (d, J = 12.3 Hz, 2 H), 1.69-1.59 (m, 4 H), 1.50 (s, 1 H), 0.96 (br, 2 H), 0.73 (d, J = 4.2 Hz, 2 H) ¹³C NMR (125 MHz, CDCl₃), δ 173.0, 164.2, 158.9, 156.0, 155.7, 149.6, 148.1, 144.9, 121.1, 120.2, 118.8, 107.8, 107.5, 100.2, 55.7, 55.2, 49.9, 46.2, 42.9, 30.2, 22.4, 17.2, 15.1, 7.2. HRMS (ESI) for $C_{30}H_{39}N_7O_3$ $[M+H]^+$, Calcd: 546.3187, Found: 546.3183, RT= 1.18 min. HPLC analysis: MeOH-H₂O (85: 15), RT= 12.76 min, 97.4% purity.

***N*-((1*S*,4*S*)-4-(2-((2-methoxy-4-(4-methylpiperazin-1-yl)phenyl)amino)-5-methyl-7-oxopyrido[2,3-*d*]pyrimidin-8(7*H*)-yl)cyclohexyl)isobutyramide (5*l*).** Compound **5l** was prepared following a similar procedure to that used for preparation of **5h**. Yellow solid, yield 75%. ¹H NMR (400 MHz, CDCl₃), δ 8.61 (s, 1 H), 8.18 (d, J = 8.5 Hz, 1 H), 7.68 (br, 1 H), 6.57-6.53 (m, 2 H), 6.24 (br, 1 H), 6.19(s, 1 H), 5.55 (br, 1 H), 4.33 (s, 1 H), 3.91(s, 3 H), 3.20 (br, 4 H), 2.74 (q, J = 13.7 Hz, 4 H), 2.61 (br, 4 H), 2.48-2.45(m, 1

H), 2.37 (s, 6 H), 1.96-1.93 (m, 4 H), 1.70-1.59 (m, 4 H), 1.22 (s, 3 H), 1.20 (s, 3 H). ^{13}C NMR (125 MHz, CDCl_3), δ 176.7, 164.2, 158.9, 156.0, 155.7, 149.6, 148.1, 144.9, 121.1, 120.2, 118.8, 107.8, 107.5, 100.2, 55.8, 55.2, 49.9, 46.2, 42.5, 35.8, 30.2, 22.2, 19.8, 17.2. HRMS (ESI) for $\text{C}_{30}\text{H}_{41}\text{N}_7\text{O}_3$ $[\text{M}+\text{H}]^+$, Calcd: 548.3344, Found: 548.3341, RT= 1.18 min. HPLC analysis: MeOH- H_2O (90: 10), RT= 10.46 min, 99.1% purity.

***N*-((1*S*,4*S*)-4-(2-((2-methoxy-4-(4-methylpiperazin-1-yl)phenyl)amino)-5-methyl-7-oxopyrido[2,3-*d*]pyrimidin-8(7*H*)-yl)cyclohexyl)pivalamide (5*m*)**. Compound **17** was prepared following a similar procedure to that used for preparation of **5h**. Yellow solid, yield 68%. ^1H NMR (400 MHz, CDCl_3), δ 8.61 (s, 1 H), 8.19 (d, $J = 8.6$ Hz, 1 H), 7.68 (s, 1 H), 6.58-6.54 (m, 2 H), 6.40 (d, $J = 8.32$ Hz, 1 H), 6.20 (s, 1 H), 5.56 (m, 1 H), 4.32-4.29 (m, 1 H), 3.91 (s, 3 H), 3.21 (t, $J = 5.0$ Hz, 4 H), 2.74 (t, $J = 13.1$ Hz, 2 H), 2.61 (t, $J = 4.9$ Hz, 4 H), 2.37 (s, 6 H), 1.94 (d, $J = 12.6$ Hz, 2 H), 1.70-1.59 (m, 4 H), 1.29 (s, 9 H). ^{13}C NMR (125 MHz, CDCl_3), δ 178.0, 164.2, 159.1, 156.0, 155.9, 149.8, 148.3, 144.7, 121.3, 119.0, 107.9, 107.6, 100.4, 55.9, 55.3, 50.0, 46.3, 42.7, 39.1, 29.9, 27.9, 22.2, 17.2. HRMS (ESI) for $\text{C}_{31}\text{H}_{43}\text{N}_7\text{O}_3$ $[\text{M}+\text{H}]^+$, Calcd: 562.3500, Found: 562.3505, RT= 3.29 min. HPLC analysis: MeOH- H_2O (90: 10), RT= 13.48 min, 97.8% purity.

***N*-((1*S*,4*S*)-4-(2-((2-methoxy-4-(4-methylpiperazin-1-yl)phenyl)amino)-5-methyl-7-oxopyrido[2,3-*d*]pyrimidin-8(7*H*)-yl)cyclohexyl)cyclopentanecarboxamide (5*n*)**. Compound **5n** was prepared following a similar procedure to that used for preparation of **5h**. Yellow solid, yield 73%. ^1H NMR (500 MHz, CDCl_3), δ 8.61 (s, 1 H), 8.18 (d, $J = 8.4$ Hz, 1 H), 7.68 (br, 1 H), 6.56-6.53 (m, 2 H), 6.21 (s, 1 H), 6.19 (s, 1 H), 5.54 (br, 1 H), 4.32 (s, 1 H), 3.90 (s, 3 H), 3.21 (t, $J = 4.25$ Hz, 4 H), 2.74 (q, $J = 11.5$ Hz, 4 H), 2.61 (t, J

= 4.35 Hz, 4 H), 2.37(s, 6 H), 2.21(s, 1 H), 1.95-1.92(m, 4 H), 1.83-1.74 (m, 4 H), 1.69-1.58 (m, 6 H). ^{13}C NMR (125 MHz, CDCl_3), δ 175.7, 164.3, 159.0, 156.0, 155.8, 149.7, 148.1, 144.8, 121.3, 120.3, 118.9, 107.9, 107.5, 100.3, 55.8, 55.2, 49.9, 46.3, 46.2, 42.7, 30.6, 30.1, 22.3, 17.2. HRMS (ESI) for $\text{C}_{32}\text{H}_{43}\text{N}_7\text{O}_3$ $[\text{M}+\text{H}]^+$, Calcd: 574.3500, Found: 574.3480, RT= 0.1 min. HPLC analysis: MeOH- H_2O (90: 10), RT= 10.09 min, 98.5% purity.

***N*-((1*S*,4*S*)-4-(2-((2-methoxy-4-(4-methylpiperazin-1-yl)phenyl)amino)-5-methyl-7-oxopyrido[2,3-*d*]pyrimidin-8(7*H*)-yl)cyclohexyl)cyclohexanecarboxamide (5o).**

Compound **5o** was prepared following a similar procedure to that used for preparation of **5h**. Yellow solid, yield 70%. ^1H NMR (500 MHz, CDCl_3), δ 8.60 (s, 1 H), 8.18 (d, J = 8.5 Hz, 1 H), 7.68 (br, 1 H), 6.56-6.53 (m, 2 H), 6.18 (s, 1 H), 6.15 (d, J = 7.1 Hz, 1 H), 5.53 (t, J = 11.9 Hz, 1 H), 4.31 (d, J = 7.6 Hz, 1 H), 3.90 (s, 3 H), 3.21 (t, J = 4.25 Hz, 4 H), 2.74 (q, J = 10.9 Hz, 4 H), 2.62 (t, J = 4.25 Hz, 4 H), 2.37(s, 3 H), 2.36 (s, 3 H), 2.16 (t, J = 11.5 Hz, 1 H), 1.91 (br, 4 H), 1.79 (d, J = 12.5 Hz, 2 H), 1.69-1.64 (m, 3 H), 1.59 (d, J = 9.7 Hz, 2 H), 1.48 (q, J = 9.7 Hz, 2 H), 1.34-1.22 (m, 4 H). ^{13}C NMR (125 MHz, CDCl_3), δ 175.6, 164.2, 158.9, 155.9, 155.7, 149.6, 148.0, 144.8, 121.1, 120.2, 118.9, 107.7, 107.4, 100.2, 55.7, 55.1, 49.8, 46.1, 45.7, 42.4, 30.1, 29.8, 25.8, 22.3, 17.2. HRMS (ESI) for $\text{C}_{33}\text{H}_{45}\text{N}_7\text{O}_3$ $[\text{M}+\text{H}]^+$, Calcd: 588.3657, Found: 588.3651, RT= 0.19 min. HPLC analysis: MeOH- H_2O (90: 10), RT= 11.58 min, 100% purity.

(3*R*,5*R*,7*R*)-*N*-((1*S*,4*S*)-4-(2-((2-methoxy-4-(4-methylpiperazin-1-yl)phenyl)amino)-5-methyl-7-oxopyrido[2,3-*d*]pyrimidin-8(7*H*)-yl)cyclohexyl)adamantane-1-carboxamide (5p). Compound **5p** was prepared following a similar procedure to that used for

preparation of **5h**. Yellow solid, yield 90%. ^1H NMR (500 MHz, CDCl_3), δ 8.61 (s, 1 H), 8.19 (d, $J = 8.3$ Hz, 1 H), 7.68 (br, 1 H), 6.57-6.54 (m, 2 H), 6.32(d, $J = 8.3$ Hz, 1 H), 6.20 (s, 1 H), 5.54 (t, $J = 12.1$ Hz, 1 H), 4.33-4.31 (m, 1 H), 3.91(s, 3 H), 3.23 (t, $J = 4.5$ Hz, 4 H), 2.75 (q, $J = 10.7$ Hz, 4 H), 2.65 (br, 4 H), 2.40(s, 3 H), 2.37(s, 3 H), 2.07(br, 3 H), 1.95-1.94(m, 7 H), 1.91 (br, 2 H), 1.75 (br, 6 H), 1.70-1.59(m, 5 H). ^{13}C NMR (125 MHz, CDCl_3), δ 177.5, 164.2, 159.0, 156.0, 155.8, 149.6, 148.1, 144.7, 121.3, 119.0, 107.9, 107.5, 107.4, 100.3, 55.8, 55.2, 49.9, 46.2, 42.3, 40.9, 39.3, 36.7, 30.1, 28.3, 22.3, 17.2. HRMS (ESI) for $\text{C}_{37}\text{H}_{49}\text{N}_7\text{O}_3$ $[\text{M}+\text{H}]^+$, Calcd: 640.3970, Found: 640.3964, RT= 0.12 min. HPLC analysis: MeOH- H_2O (90: 10), RT= 16.55 min, 96.7% purity.

***N*-((1*S*,4*S*)-4-(2-((2-methoxy-4-(4-methylpiperazin-1-yl)phenyl)amino)-5-methyl-7-oxopyrido[2,3-*d*]pyrimidin-8(7*H*)-yl)cyclohexyl)benzamide (5q)**. Compound **5q** was prepared following a similar procedure to that used for preparation of **5h**. Yellow solid, yield 84%. ^1H NMR (500 MHz, CDCl_3), δ 8.62 (s, 1 H), 8.20 (d, $J = 6.8$ Hz, 1 H), 7.95 (d, $J = 6.8$ Hz, 1 H), 7.70 (s, 1 H), 7.49-7.47 (m, 3 H), 6.97 (br, 1 H), 6.58-6.56 (m, 2 H), 6.22(s, 1 H), 5.63 (m, 1 H), 4.57 (s, 1 H), 3.91(s, 3 H), 3.23 (br, 4 H), 2.87 (q, $J = 12.6$ Hz, 2 H), 2.63 (br, 4 H), 2.38(s, 3 H), 2.39(s, 6 H), 2.08 (d, $J = 12.7$ Hz, 2 H), 1.99 (br, 1 H), 1.77 (t, $J = 13.7$ Hz, 2 H), 1.67 (d, $J = 12.4$ Hz, 2 H). ^{13}C NMR (125 MHz, CDCl_3), δ 166.9, 164.2, 159.0, 156.1, 155.8, 149.7, 148.2, 144.8, 135.0, 131.4, 128.7, 127.2, 121.2, 118.9, 107.9, 107.5, 100.3, 55.8, 55.2, 50.0, 46.2, 43.4, 30.1, 22.2, 17.2. HRMS (ESI) for $\text{C}_{33}\text{H}_{39}\text{N}_7\text{O}_3$ $[\text{M}+\text{H}]^+$, Calcd: 582.3187, Found: 582.03186, RT= 0.11 min. HPLC analysis: MeOH- H_2O (90: 10), RT= 9.42 min, 95.2% purity.

***N*-((1*S*,4*S*)-4-(2-((2-methoxy-4-(4-methylpiperazin-1-yl)phenyl)amino)-5-methyl-7-**

-oxopyrido[2,3-*d*]pyrimidin-8(7*H*)-yl)cyclohexyl)-1-naphthamide (5r). To a solution of HATU (228 mg, 0.6 mmol) and DIEA (0.1 ml, 0.8 mmol) in DMF (5ml) was added 1-Naphthoic acid (112 mg, 0.7 mmol). The reaction mixture was stirred at room temperature for 30 minutes, and **19h** (238.8 mg, 0.5 mmol) was added to the stirring mixture, and stirred at room temperature for 2hrs until the reaction was completed, as monitored by TLC. The mixture was diluted with DCM, and washed with H₂O for 5 times. The organic layer was dried with Na₂SO₄, and concentrated *in vacuo*. The residue was purified by flash column chromatography (SiO₂, 1 - 10% MeOH in DCM) to give **5r** (yellow solid, 70 mg, yield 77%). ¹H NMR (500 MHz, CDCl₃), δ 8.59 (s, 1 H), 8.40 (d, *J* = 8.5 Hz, 1 H), 8.22 (s, 1 H), 7.90 (d, *J* = 7.9 Hz, 1 H), 7.86 (d, *J* = 8.1 Hz, 1 H), , 7.75 (d, *J* = 6.9 Hz, 1 H), 7.71 (br, 1 H), 7.57 (t, *J* = 7.1 Hz, 1 H), 7.51 (t, *J* = 7.5 Hz, 1 H), 6.74 (d, *J* = 7.4 Hz, 1 H), 6.58-6.57(m, 2 H), 6.13 (s, 1 H), 5.59 (t, *J* = 11.6 Hz, 1 H), 4.65-4.63 (m, 1 H), 3.91(s, 3 H), 3.24 (br, 4 H), 2.86 (q, *J* = 11.9 Hz, 2 H), 2.65 (t, *J* = 4.3 Hz, 4 H), 2.40 (s, 3 H), 2.33 (s, 3 H), 2.20 (d, 2 *J* = 13.6 Hz, 2 H), 1.84 (q, *J* = 13.9 Hz, 2 H), 1.68 (d, *J* = 12.0 Hz, 2 H). ¹³C NMR (125 MHz, CDCl₃), δ 169.2, 164.2, 159.0, 156.0, 155.8, 148.2, 144.8, 134.8, 133.9, 130.7, 130.5, 128.4, 127.2, 126.4, 125.7, 125.3, 125.1, 121.3, 118.9, 107.9, 107.5, 100.3, 55.8, 55.3, 53.5, 50.0, 46.2, 43.8, 30.4, 22.8, 17.2. HRMS (ESI) for C₃₇H₄₁N₇O₃ [M+H]⁺, Calcd: 632.3344, Found: 632.3339, RT= 0.2 min. HPLC analysis: MeOH-H₂O (90: 10), RT= 10.40 min, 99.2% purity.

8-((1*S*,4*S*)-4-((cyclopropylmethyl)amino)cyclohexyl)-2-((2-methoxy-4-(4-methylpiperazin-1-yl)phenyl)amino)-5-methylpyrido[2,3-*d*]pyrimidin-7(8*H*)-one (5s). To a solution of **19h** (300 mg, 0.6 mmol) and AcOH (72 μl, 1.3 mmol) in anhydrous THF was

added Cyclopropanecarboxaldehyde (56 μ l, 0.8 mmol) and 4 \AA molecular sieves. The reaction mixture was stirred at room temperature for 4 hrs under argon. Sodium triacetoxyborohydride (266 mg, 1.3 mmol) was added, and the mixture was stirred at room temperature for another 4 hrs. The mixture was then filtered through celite, and the organic layer was concentrated *in vacuo*. The residue was purified by flashing column chromatography (SiO₂, 1 - 10% MeOH in DCM) to give **5s** (yellow solid, 35 mg, yield 11%). ¹H NMR (400 MHz, CDCl₃), δ 8.61 (s, 1 H), 8.18 (d, J = 7.2 Hz, 1 H), 7.66 (s, 1 H), 6.57-6.54 (m, 2 H), 6.20 (s, 1 H), 5.49 (s, 1 H), 3.90 (s, 3 H), 3.20 (t, J = 4.7 Hz, 4 H), 3.05 (s, 1 H), 2.80 (q, J = 13.0 Hz, 2 H), 2.61 (t, J = 4.8 Hz, 4 H), 2.54 (d, J = 6.8 Hz, 2 H), 2.37 (s, 3 H), 2.36 (s, 3 H), 2.32 (br, 3 H), 2.08 (d, J = 13.2 Hz, 2 H), 1.61 (t, J = 13.9 Hz, 2 H), 1.52 (d, J = 12.3 Hz, 2 H), 1.11 (m, 1 H), 0.87 (m, 1 H), 0.55 (d, J = 7.5 Hz, 2 H), 0.21 (d, J = 3.2 Hz, 2 H). ¹³C NMR (125 MHz, DMSO-*d*₆), δ 162.8, 159.6, 156.6, 155.1, 152.3, 149.1, 145.3, 124.3, 119.4, 117.1, 106.6, 106.3, 99.9, 55.5, 54.5, 52.3, 50.9, 50.1, 48.5, 45.6, 28.7, 22.2, 16.6, 9.9, 3.5. HRMS (ESI) for C₃₀H₄₁N₇O₂ [M+H]⁺, Calcd: 532.3395, Found: 532.3394, RT= 2.79 min. HPLC analysis: MeOH-H₂O (90 :10), RT= 26.64 min, 96.3% purity.

***N*-((1*S*,4*S*)-4-(2-((2-methoxy-4-(4-methylpiperazin-1-yl)phenyl)amino)-7-oxopyridin-2,3-*d*]pyrimidin-8(7*H*)-yl)cyclohexyl)propionamide (5*t*)**. Compound **5t** was prepared following a similar procedure to that used for preparation of **5h**. Yellow solid, yield 78%. ¹H NMR (400 MHz, CDCl₃), δ 8.50 (s, 1 H), 8.18 (d, J = 8.6 Hz, 1 H), 7.71 (s, 1 H), 7.47 (d, J = 9.3 Hz, 1 H), 6.58-6.54 (m, 2 H), 6.36 (d, J = 9.3 Hz, 1 H), 6.23 (s, 1 H), 5.57 (m, 1 H), 4.36-4.34 (m, 1 H), 3.92 (s, 3 H), 3.21 (t, J = 4.8 Hz, 4 H), 2.79-2.70 (m, 2 H), 2.61

(t, $J = 5.0$ Hz, 4 H), 2.38 (s, 3 H), 2.30 (q, $J = 7.6$ Hz, 2 H), 1.96 (d, $J = 13.0$ Hz, 2 H), 1.72-1.68 (m, 2 H), 1.61 (s, 2 H), 1.22 (t, $J = 7.6$ Hz, 3 H). ^{13}C NMR (125 MHz, CDCl_3), δ 173.5, 164.5, 159.0, 158.6, 155.9, 149.8, 148.3, 135.8, 121.1, 120.4, 119.4, 107.8, 106.9, 100.2, 58.4, 55.9, 55.3, 49.9, 46.3, 42.7, 31.7, 31.6, 30.2, 30.1, 29.8, 22.2, 18.6, 14.2, 10.2. HRMS (ESI) for $\text{C}_{28}\text{H}_{37}\text{N}_7\text{O}_3$ $[\text{M}+\text{H}]^+$, Calcd: 520.3031, Found: 520.3045, RT= 2.98 min. HPLC analysis: MeOH- H_2O (90:10), RT= 9.21 min, 100% purity.

***N*-((1*S*,4*S*)-4-(5-ethyl-2-((2-methoxy-4-(4-methylpiperazin-1-yl)phenyl)amino)-7-oxopyrido[2,3-*d*]pyrimidin-8(7*H*)-yl)cyclohexyl)propionamide (5u)**. Compound **5u** was prepared following a similar procedure to that used for preparation of **5h**. Yellow solid, yield 88%. ^1H NMR (400 MHz, CDCl_3), δ 8.67 (s, 1 H), 8.18 (d, $J = 8.7$ Hz, 1 H), 7.66 (s, 1 H), 6.58-6.53 (m, 2 H), 6.28 (s, 1 H), 6.22 (s, 1 H), 5.59-5.53 (m, 1 H), 4.36-4.34 (m, 1 H), 3.92 (s, 3 H), 3.49 (s, 1H), 3.21 (t, $J = 4.8$ Hz, 4 H), 2.80-2.69 (m, 4 H), 2.61 (t, $J = 5.0$ Hz, 4 H), 2.37 (s, 3 H), 2.31 (q, $J = 7.6$ Hz, 2 H), 1.95 (d, $J = 14.2$ Hz, 2 H), 1.72-1.67 (m, 2 H), 1.60 (s, 2 H), 1.31 (t, $J = 7.4$ Hz, 3 H), 1.22 (t, $J = 7.6$ Hz, 3 H). ^{13}C NMR (125 MHz, CDCl_3), δ 173.5, 164.5, 158.8, 155.9, 155.7, 150.3, 149.7, 148.2, 121.2, 120.3, 116.8, 107.8, 106.7, 100.3, 99.8, 55.8, 55.2, 55.1, 49.9, 46.2, 42.7, 30.2, 30.1, 29.8, 23.5, 22.3, 12.9, 10.2. HRMS (ESI) for $\text{C}_{30}\text{H}_{41}\text{N}_7\text{O}_3$ $[\text{M}+\text{H}]^+$, Calcd: 548.3344, Found: 548.3341, RT= 3.15 min. HPLC analysis: MeOH- H_2O (90: 10), RT= 12.51 min, 98.8% purity.

***N*-((1*S*,4*S*)-4-(2-((2-methoxy-4-(4-methylpiperazin-1-yl)phenyl)amino)-7-oxo-5-phenylpyrido[2,3-*d*]pyrimidin-8(7*H*)-yl)cyclohexyl)propionamide (5w)**. Compound **5w** was prepared following a similar procedure to that used for preparation of **5v**. Yellow

solid, yield 50% ^1H NMR (500 MHz, CDCl_3), δ 8.51 (s, 1 H), 8.23 (d, $J = 8.0$ Hz, 1 H), 7.72 (s, 1 H), 7.50 (br, 3 H), 7.43 (br, 2 H), 6.57-6.56 (m, 2 H), 6.32 (s, 1 H), 6.27 (s, 1 H), 5.63 (br, 1 H), 4.38 (br, 1 H), 3.92 (s, 3 H), 3.34 (br, 4 H), 2.90 (br, 4 H), 2.81 (q, $J = 13.8$ Hz, 2 H), 2.57 (s, 3 H), 2.32 (q, $J = 7.2$ Hz, 3 H), 1.99 (d, $J = 12.8$ Hz, 4 H), 1.74-1.71 (m, 7 H), 1.23-1.22 (m, 3 H). ^{13}C NMR (125 MHz, CDCl_3), δ 173.7, 164.0, 158.3, 149.7, 147.4, 135.4, 129.5, 129.0, 128.8, 122.2, 118.6, 108.9, 100.7, 55.9, 54.7, 49.2, 42.8, 30.3, 30.2, 29.8, 22.8, 22.3, 14.3, 10.2. HRMS (ESI) for $\text{C}_{31}\text{H}_{41}\text{N}_7\text{O}_3$ $[\text{M}+\text{H}]^+$, Calcd: 596.3271, Found: 596.3347. HPLC analysis: MeOH- H_2O (90: 10), RT= 12.25 min, 98.4% purity.

***N*-((1*S*,4*S*)-4-(2-((2-methoxy-4-(4-methylpiperazin-1-yl)phenyl)amino)-6-methyl-7-oxopyrido[2,3-*d*]pyrimidin-8(7*H*)-yl)cyclohexyl)propionamide (5x).** Compound **5x** was prepared following a similar procedure to that used for preparation of **5h**. Yellow solid, yield 63%. ^1H NMR (500 MHz, CDCl_3), δ 8.45 (s, 1 H), 8.20 (d, 1 H, $J = 8.6$ Hz), 7.65 (s, 1 H), 7.35 (s, 1 H), 6.57-6.53 (m, 2 H), 6.25 (s, 1 H), 5.57 (m, 1 H), 4.35-4.34 (m, 1 H), 3.91 (s, 3 H), 3.21 (t, $J = 4.7$ Hz, 4 H), 2.77 (q, $J = 11.1$ Hz, 2 H), 2.62 (t, $J = 4.8$ Hz, 4 H), 2.37 (s, 3 H), 2.30 (q, $J = 7.6$ Hz, 2 H), 2.16 (s, 3 H), 1.96 (d, $J = 13.8$ Hz, 2 H), 1.78 (s, 6 H), 1.74-1.68 (m, 2 H), 1.61 (d, $J = 12.6$ Hz, 2 H), 1.21 (t, $J = 7.6$ Hz, 3 H). ^{13}C NMR (125 MHz, CDCl_3), δ 173.5, 164.9, 158.4, 157.5, 155.1, 149.6, 148.0, 132.4, 127.6, 121.4, 120.1, 107.9, 107.0, 100.3, 55.8, 55.2, 50.0, 46.2, 42.8, 32.0, 30.3, 30.2, 29.8, 22.8, 22.5, 17.2, 14.2, 10.2. HRMS (ESI) for $\text{C}_{29}\text{H}_{39}\text{N}_7\text{O}_3$ $[\text{M}+\text{H}]^+$, Calcd: 534.3187, Found: 534.3183, RT= 1.2 min. HPLC analysis: MeOH- H_2O (85: 15), RT= 10.54 min, 98.4%

***N*-((1*S*,4*S*)-4-(2-((2-methoxy-4-(4-methylpiperazin-1-yl)phenyl)amino)-6-methyl-7-oxopyrido[2,3-*d*]pyrimidin-8(7*H*)-yl)cyclohexyl)cyclopentanecarboxamide (5y).**

Compound **5y** was prepared following a similar procedure to that used for preparation of **5r**. Yellow solid, yield 65%. ^1H NMR (400 MHz, CDCl_3), δ 8.45 (s, 1 H), 8.21 (d, $J = 8.2$ Hz, 1 H), 7.65 (s, 1 H), 7.35 (s, 1 H), 6.57-6.54 (m, 2 H), 6.18 (br, 1 H), 5.57 (m, 1 H), 4.35-4.33 (m, 1 H), 3.91 (s, 3 H), 3.24 (t, $J = 4.7$ Hz, 4 H), 2.78 (q, $J = 12.9$ Hz, 2 H), 2.67 (t, $J = 4.5$ Hz, 4 H), 2.62-2.6(m, 1 H), 2.41 (s, 3 H), 2.17 (s, 3 H), 1.98-1.67 (m, 14 H). ^{13}C NMR (125 MHz, CDCl_3), δ 175.9, 164.9, 158.3, 157.4, 155.0, 149.5, 147.9, 132.3, 127.5, 121.4, 120.1, 107.9, 106.9, 100.3, 55.7, 55.1, 53.4, 49.9, 46.1, 42.7, 30.6, 30.3, 29.7, 26.0, 22.5, 17.1. HRMS (ESI) for $\text{C}_{32}\text{H}_{43}\text{N}_7\text{O}_3$ $[\text{M}+\text{H}]^+$, Calcd: 574.3500, Found: 574.3491, RT= 0.1 min. HPLC analysis: MeOH- H_2O (90: 10), RT= 11.78 min, 97.5% purity.

N-((1*S*,4*S*)-4-(2-((2-methoxy-4-(4-methylpiperazin-1-yl)phenyl)amino)-6-methyl-7-oxopyrido[2,3-*d*]pyrimidin-8(7*H*)-yl)cyclohexyl)cyclohexanecarboxamide (**5z**).

Compound **5z** was prepared following a similar procedure to that used for preparation of **5h**. Yellow solid, yield 68%. ^1H NMR (400 MHz, CDCl_3), δ 8.43 (s, 1 H), 8.19 (d, $J = 7.9$ Hz, 1 H), 7.65 (s, 1 H), 7.34 (s, 1 H), 6.56-6.52 (m, 2 H), 6.12 (d, $J = 7.5$ Hz, 1 H), 5.56 (m, 1 H), 4.33 (br, 1 H), 3.89 (s, 3 H), 3.21 (br, 4 H), 2.76 (q, $J = 12.6$, 2 H), 2.63 (br, 4 H), 2.38 (s, 3 H), 2.15 (s, 3 H), 1.92 (t, $J = 15.6$ Hz, 4 H), 1.79 (d, $J = 10.0$ Hz, 2 H), 1.73-1.66 (m, 2 H), 1.60 (d, $J = 12.6$ Hz, 2 H), 1.50 (q, $J = 12.0$ Hz, 2 H), 1.32-1.24(m, 4 H). ^{13}C NMR (125 MHz, CDCl_3), δ 175.7, 164.9, 158.3, 157.4, 155.0, 149.5, 147.9, 132.3, 127.5, 121.4, 120.1, 107.9, 106.9, 100.3, 55.8, 55.8, 55.1, 53.4, 49.9, 46.1, 45.8, 42.5, 30.3, 29.8, 25.8, 22.5, 17.1. HRMS (ESI) for $\text{C}_{32}\text{H}_{43}\text{N}_7\text{O}_3$ $[\text{M}+\text{H}]^+$, Calcd: 588.3657, Found: 588.3639, RT= 0.1 min. HPLC analysis: MeOH- H_2O (90: 10), RT= 13.08 min,

97.1% purity.

Computational Study. Molecular docking was performed using Maestro 11.7 (Schrödinger LLC). The crystal structures of TTK and EGFR^{L858R/T790M} protein were taken from the Protein Data Bank (PDB code: 5EH0, 5GMP). The proteins were processed using the “Protein Preparation Wizard” workflow in Maestro 11.7 (Schrodinger LLC) to add bond orders and hydrogens. Missing side chains and loops were filled in using Prism. All heteroatom residues and crystal water molecules beyond 5 Å from a heteroatom group (protein) were removed. Hydroxyl, Asn, Gln and His states were automatically optimized using ProtAssign with default parameters. A restrained minimization job with heavy atoms restrained (or frozen) and hydrogens unrestrained was ran with default parameters. 3D structures of the inhibitors were prepared using LigPrep module with OPLS3e force field. Glide module was used as the docking program. The grid-enclosing box was placed on the centroid of the binding ligand in the optimized crystal structure as described above, and a scaling factor of 0.8 was set to van der Waals (vdW) radius of those receptor atoms with partial atomic charges of less than 0.15. Extra precision (XP) approach of Glide was adopted to dock compounds into TTK or EGFR with the default parameters. The figures were generated using PyMol. The top-ranking pose of compound **50** docking into TTK was chosen as the initial model for further molecular dynamics study. The structure of **50** was optimized, and the electrostatic potential was calculated at HF/6-31G level using GAMESS program [62]. Then, atomic partial charges were obtained by the RESP approach [63]. Amber ff99 force fields were used for protein and ions, and TIP3P was used for water molecules. Water molecules

were placed around the complex model with an encompassing distance of 8 Å to form an $85 \times 80 \times 70 \text{ \AA}^3$ periodic box, including roughly 14,000 water molecules. Charge-neutralizing ions were added to neutralize the system. Molecular Dynamics (MD) simulations were carried out in periodic boundary conditions using GROMACS program v. 5.1.4 [64]. Electrostatic interactions were calculated using the particle mesh Ewald method with a cutoff radius of 10 Å. Van der Waals interactions were cut off at 10 Å. After each of the fully solvated systems was energy minimized, the system was equilibrated for 100 ps under constant volume (NVT), and run for 100 ps under constant pressure and temperature (NPT), with positional restraints on protein heavy atoms and compound atoms. Production runs were conducted under the NPT condition without the positional restraints. In this procedure, the temperature was maintained at 298 K using velocity rescaling with a stochastic term, and the pressure was maintained at 1 bar with the Parrinello-Rahman pressure coupling, where the time constants for the temperature and pressure couplings to the bath were 0.1 and 2 ps, respectively. 30 ns production run was performed for the protein-ligand complex system (TTK-**5o**). Equilibration and production runs were performed with time steps of 2 fs, and snapshots were output every 2 ps to yield 500 snapshots per nanosecond of simulation. The binding free energy between TTK and **5o** was calculated by MM-PBSA (Molecular Mechanics Poisson-Boltzmann Surface Area) [65] to evaluate the contribution of each residue of the system to the total binding free energy. The coordinate trajectories were saved every 2 ps during the sampling process. The binding free energy (ΔG_{bind}) was performed using the generated stable conformations from last 5 ns.

***In Vitro* Kinase Assay.** All the binding affinities (K_d) and kinome selectivity profiles (KINOMEscan profiling) were conducted by Eurofins DiscoveryX Corporation (San Diego, CA, USA) by following the previous described protocols [66]. The data are mean values from two independent experiments with variation less than 15%. Briefly, kinases were tagged with DNA for qPCR detection, while the biotinylated small molecule ligands were immobilized to streptavidin-coated magnetic beads. Compounds that bind to the kinase active prevent kinase binding to the immobilized ligand. Thus, “hits” of KINOMEscan profiling could be identified by measuring the amount of kinase captured in test versus control samples by using a quantitative, precise and ultra-sensitive qPCR method that detects the associated DNA label. In a similar manner, K_d values for test compound-kinase interaction are calculated by measuring the amount of kinase captured on the solid support as a function of the test compound concentration. The enzyme potency test (IC_{50}) was conducted by Eurofins Cerep SA (France). TTK protein was diluted in buffer (20 mM MOPS, 1 mM EDTA, 0.01% Brij-35, 5% Glycerol, 0.1% β -mercaptoethanol and 1 mg/mL BAS) prior to the reaction mix. TTK protein was then incubated with 8 mM MOPS pH 7.0, 0.2 mM EDTA, 0.33 mg/mL MBP, 10 mM Magnesium acetate and 10 μ M [γ - 33 P-ATP]. The reaction is initiated by the addition of the Mg/ATP mix. After incubation for 40 minutes at room temperature, the reaction is stopped by the addition of phosphoric acid to a concentration of 0.5%. 10 μ L of the reaction is then spotted onto a P30 filtermat and washed four times for 4 minutes in 0.425% phosphoric acid and once in methanol prior to drying and scintillation counting.

Cellular Proliferation Assays. Tumor cells were plated into 96-well plates (3000

cell/well) in RPMI-1640 (Gibico) supplemented with 10% fetal bovine serum (BI) and Pen-Strep Solution (100 units/ml Penicillin and 100 ug/ml Streptomycin, BI). After incubation overnight, the cells were treated with various concentrations (0.000508—10 μ M) of the test compounds for 96 hrs. Cell proliferation was evaluated by Cell Counting Kit 8 (CCK8, B34306, Bimake). IC₅₀ values were calculated by concentration -response curve-fitting using GraphPad Prism 5.0 software. Each IC₅₀ value was expressed as mean \pm SD.

Western Blot Analysis. HCT-116 colorectal cancer cells were treated with various concentrations of compound for designated time. Then cells were lysed in using 1 \times SDS sample lysis buffer (CST recommended) with protease and phosphatase inhibitors. Cell lysates were loaded and electrophoresed onto 8-12% SDS-PAGE gel, and then separated proteins were transferred to a PVDF film. The film was blocked with 5% fat-free milk in TBS solution containing 0.5% Tween-20 for 4 hrs at room temperature, then incubated with corresponding primary antibody (1:1000-1:200) overnight at 4 °C. After washing with TBST, HRP-conjugated secondary antibody was incubated for 2 hrs. And the protein signals were visualized by ECL Western Blotting Detection Kit (Thermo Scientific, USA), and detected with Amersham Imager 600 system (GE, America).

Immunofluorescence. The HCT-116 colorectal cancer cells were seeded into cell culture dishes (627870, Greiner) which were placed into four-well chamber slides in advance. Following treatment with or without **5o** (111.1, 333.3 nM) for 48 hrs, the cells were fixed with 4% paraformaldehyde for 15 minutes, permeabilized with 0.5% Triton X-100 for 10 minutes, blocked with 3% normal goat serum albumin for 1 hr at room

temperature and incubated with anti- β -tubulin (2146S, CST) and anti-CENP-B (SC-376283, SantaCruz) antibody at room temperature for 1 hr. Subsequently, the cells were rinsed thoroughly with PBST, and were incubated with Alexa Fluor 667-conjugated goat anti-rabbit IgG (ab97077, abcam) or Alexa Fluor 528-conjugated goat anti-mouse IgG (ab6785, abcam) for 1 hr at room temperature in the dark. ProLong Gold antifade reagent (P36931; Invitrogen, USA) was used to stain the nuclei for 5 minutes at room temperature. The cells were visualized by Laser scanning confocal microscope (Zeiss710; Germany).

Cell Cycle Analysis. After 48-hrs treatment with **5o** or DMSO, cells were harvested and washed twice with PBS. Approximately 6×10^5 cells were re-suspended in 150 μ L BD Cytotfix/Cytoperm buffer solution (#554722, BD). After 20 minutes at 4 $^{\circ}$ C, the cells were washed twice with BD Perm/Wash buffer (#554723, BD) and incubated with 200 μ l of dyeing buffer (containing 0.1 mg/ml propidium iodide, 2 mg/ml RNaseA) in the dark for 20 minutes at 4 $^{\circ}$ C. The cells were then analyzed on a Guava easyCyte flow cytometer (Merck, Whitehouse Station, NJ, USA).

Cell Apoptosis Analysis. After 48-hr treatment with **5o** or DMSO, cells were harvested and washed twice with ice-cold PBS. Approximately 6×10^5 cells were re-suspended in 100 μ L 1 \times BD Binding buffer solution (#556454, BD), and then incubated with Annexin V-PE (#556422, BD) and 7-ADD(#559925, BD) in the dark for 15 minutes. Finally, 400 μ L 1 \times BD Binding buffer solution were replenished. The cells were then analyzed on a Guava easyCyte flow cytometer (Merck, Whitehouse Station, NJ,

USA).

Pharmacokinetic Studies. All the pharmacokinetic studies were carried out by Shanghai Medicilon Inc., according to the protocols and guidelines of the institutional care and use committee. All the procedures related to animal handling, care, and treatment in this article were performed in compliance with Agreement of the Ethics Committee on Laboratory Animal Care and the Guidelines for the Care and Use of Laboratory Animals in Shanghai, China. Compound **5o** was dissolved in mixed solvents (5% DMA, 10% Solutol and 85% Saline) for intravenous injection and oral administration, with the final concentrations of 1.0 and 2.5 mg/ml respectively. SD rats (male, 3 animals per group) were injected solution of **5o** intravenously at a dose of 5 mg/kg. Jugular vein blood (0.25 ml per time) was collected at 0.083 hr, 0.25 hr, 0.5 hr, 1 hr, 2 hrs, 4 hrs, 6 hrs, 8 hrs and 24 hrs after dose administration. Blood samples was added heparin sodium and then centrifuged at 6800 g/min for 6 minutes and stored at -80 °C until further use. An aliquot of 10 µL plasma sample was protein precipitated with 1000 µL MeOH in which contains 100 ng/mL IS. The mixture was vortexed for 1 minute and centrifuged at 18000 g for 7 minutes. Transfer 200 µL supernatant to 96 well plates. An aliquot of 1 µL supernatant was injected for LC-MS/MS analysis. Data of **5o** through oral administration was collected using similar procedure of intravenous test except the dosage was increased to 25 mg/kg and the blood sample was collected at 0.5 hr, 1 hr, 2 hrs, 4 hrs, 6 hrs, 8 hrs, 10 hrs and 24 hrs after oral administration. The pharmacokinetic parameters were calculated using WinNolin and WastonLim sofeware.

***In Vivo* Efficacy Study.** Male CB17-SCID mice were purchased from Vital River

Laboratory Animal Technology Inc. (Beijing, China). All animal experiments were carried out under protocols approved by the Institutional Animal Care and Use Committee of the medical college of Jinan University. 5×10^6 HCT-116 cells were injected subcutaneously in the right flank of the SCID mice. Mice were randomly grouped based on the tumor volume when the mean tumor volume reached 100-200 mm³. Compound **50** was dissolved in 0.5% CMCNa aqueous solution for oral administration., with concentration of 5 mg/ml. Paclitaxel was dissolved in 10% cremophor solution ($V_{\text{cremophor/ethanol}} = 3/1$) in saline for intraperitoneal injection, with concentration of 2 mg/ml. The animals were treated with mono- or combined- treatment of **50** (50 mg/kg, po, 2 days on/4 days off) and paclitaxel (20 mg/kg, ip, QW). The same dose of CMCNa aqueous solution and cremophor aqueous solution was use as vehicle treatment. Tumor volume and body weight were monitored every 2 days. Tumor volume (TV) were calculated as $TV = L \times W^2 / 2$ (L and W are the length and width of the tumor, respectively). Tumor growth inhibition were calculated as : $TGI = [1 - (T - T_0) / (C - C_0)] \times 100$ (T and T₀ are final and initial tumor volumes of compound treated group, respectively; C and C₀ are final and initial tumor volumes of control group, respectively). Body weight loss were calculated as : $BWL = (W - W_0) / W_0 \times 100$ (W and W₀ are final and initial body weight of mice, respectively).

Declaration of competing interest

The authors declare no competing financial interest.

ACKNOWLEDGMENT

The authors appreciate the financial support from National Natural Science Foundation of China (81820108029, 81874284, 21572230, 81673285 and 81425021), Guangdong Province (2015A030312014, 2018B030337001, 2015A030306042, 2016A050502041), Guangzhou city (201805010007) and Jinan University.

ABBREVIATIONS

APC/C, Anaphase Promoting Complex; BWL, Body Weight Loss; CIN, Chromosomal Instability; CENP-B, Centromere Protein B; DAPI, 4',6-diamidino-2-phenylindole; DCM, Dichloromethane; DMF, *N,N*-Dimethylformamide; DIEA, *N,N*-Diisopropylethylamine; EGFR, Epidermal Growth Factor Receptor; EA, Ethyl Acetate; eq., Equiv; Knl1, Kinetochore Null Protein 1; HATU, 2-(7-aza-1H-benzotriazol-1-yl)-1,1,3,3-tetramethyluronium hexafluorophosphate; H-bond, Hydrogen-bond; LiAlH₄, Lithium Aluminum Hydride; MCC, Mitotic Checkpoint Complex; MnO₂, Manganese Dioxide; MTD, Maximal Tolerance Dose; POC, Percent Of Control; SAC, Spindle Assembly Checkpoint; siRNA, Small Interfering RNA; rt, Room Temperature; TFA, Trifluoroethanoic acid; TGI, Tumor Growth Inhibition; THF, Tetrahydrofuran. TTK, Threonine Tyrosine Kinase.

REFERENCES

- [1] M. Winey, L. Goetsch, P. Baum, B. Byers, Mps1 and Mps2 - Novel Yeast Genes Defining Distinct Steps of Spindle Pole Body Duplication, *J. Cell Biol.* 114 (1991) 745-754. <https://doi.org/10.1083/jcb.114.4.745>.
- [2] A. Musacchio, *The Molecular Biology of Spindle Assembly Checkpoint Signaling*

- Dynamics, *Curr. Biol.* 25 (2015) 1002-1018. <https://doi.org/10.1016/j.cub.2015.10.050>.
- [3] N. London, S. Biggins, Signalling dynamics in the spindle checkpoint response, *Nat. Rev. Mol. Cell Biol.* 15 (2014) 736-747. <https://doi.org/10.1038/nrm3888>.
- [4] S. Santaguida, A. Amon, Short- and long-term effects of chromosome mis-segregation and aneuploidy, *Nat. Rev. Mol. Cell Bio.* 16 (2015) 473. <https://doi.org/10.1038/nrm4025>.
- [5] Z. Dou, D. K. Prifti, P. Gui, X. Liu, S. Elowe, X. Yao, Recent Progress on the Localization of the Spindle Assembly Checkpoint Machinery to Kinetochores. *Cells* 8 (2019) 278. <https://doi.org/10.3390/cells8030278>.
- [6] S.T. Pachis, G. Kops, 2018. Leader of the SAC: molecular mechanisms of Mps1/TTK regulation in mitosis, *Open Biol.* 8, 180109. <https://doi.org/10.1098/rsob.180109>.
- [7] W.C. Chao, K. Kulkarni, Z. Zhang, E.H. Kong, D. Barford, Structure of the mitotic checkpoint complex, *Nature.* 484 (2012) 208-213. <https://doi.org/10.1038/nature10896>.
- [8] E.A. Foley, T.M. Kapoor, Microtubule attachment and spindle assembly checkpoint signalling at the kinetochore, *Nat. Rev. Mol. Cell Biol.* 14 (2013) 25-37. <https://doi.org/10.1038/nrm3494>.
- [9] C. Kasbek, C.-H. Yang, A.M. Yusof, H.M. Chapman, M. Winey, H.A. Fisk, Preventing the degradation of Mps1 at centrosomes is sufficient to cause centrosome reduplication in human cells, *Mol. Biol. Cell.* 18 (2007) 4457-4469. <https://doi.org/10.1091/mbc.E07-03-0283>.
- [10] C. Kasbek, C.H. Yang, H.A. Fisk, Mps1 as a link between centrosomes and genomic instability, *Environ. Mol. Mutagen.* 50 (2009) 654-665.

<https://doi.org/10.1002/em.20476>.

[101] H.A. Fisk, C.P. Mattison, M. Winey, Human Mps1 protein kinase is required for centrosome duplication and normal mitotic progression, *Proc. Natl. Acad. Sci. U. S. A.* 100 (2003) 14875-14880. <https://doi.org/10.1073/pnas.2434156100>.

[12] J.H. Wei, Y.F. Chou, Y.H. Ou, Y.H. Yeh, S.W. Tyan, T.P. Sun, C.Y. Shen, S.Y. Shieh, TTK/hMps1 participates in the regulation of DNA damage checkpoint response by phosphorylating CHK2 on threonine 68, *J. Biol. Chem.* 280 (2005) 7748-7757. <https://doi.org/10.1074/jbc.M410152200>.

[13] A. Janssen, M. van der Burg, K. Szuhai, G.J. Kops, R.H. Medema, Chromosome segregation errors as a cause of DNA damage and structural chromosome aberrations, *Science*, 333 (2011) 1895-1898. <https://doi.org/10.1126/science.1210214>.

[14] K. Nihira, N. Taira, Y. Miki, K. Yoshida, TTK/Mps1 controls nuclear targeting of c-Abl by 14-3-3-coupled phosphorylation in response to oxidative stress, *Oncogene*, 27 (2008) 7285-7295. <https://doi.org/10.1038/onc.2008.334>.

[15] Y.-F. Huang, M.D.-T. Chang, S.-Y. Shieh, TTK/hMps1 Mediates the p53-Dependent Postmitotic Checkpoint by Phosphorylating p53 at Thr18, *Mol. Cell. Biol.* 29 (2009) 2935-2944. <https://doi.org/10.1128/mcb.01837-08>.

[16] Z.-C. Yu, Y.-F. Huang, S.-Y. Shieh, Requirement for human Mps1/TTK in oxidative DNA damage repair and cell survival through MDM2 phosphorylation, *Nucleic Acids Res.* 44 (2016) 1133-1150. <https://doi.org/10.1093/nar/gkv1173>.

[17] S. Majumder, H.A. Fisk, VDAC3 and Mps1 negatively regulate ciliogenesis, *Cell Cycle*, 12 (2013) 849-858. <https://doi.org/10.4161/cc.23824>.

- [18] R.E. Meyer, J. Brown, L. Beck, D.S. Dawson, Mps1 promotes chromosome meiotic chromosome biorientation through Dam1, *Mol. Biol. Cell.* 29 (2018) 479-489. <https://doi.org/10.1091/mbc.E17-08-0503>.
- [19] W. El Yakoubi, E. Buffin, D. Cladiere, Y. Gryaznova, I. Berenguer, S.A. Touati, R. Gomez, J.A. Suja, J.M. van Deursen, K. Wassmann, Mps1 kinase-dependent Sgo2 centromere localisation mediates cohesin protection in mouse oocyte meiosis I, *Nat. Commun.* 8 (2017) 694. <https://doi.org/10.1038/s41467-017-00774-3>.
- [20] L.H. Saal, S.K. Gruvberger-Saal, C. Persson, K. Lovgren, M. Jumppanen, J. Staaf, G. Jonsson, M.M. Pires, M. Maurer, K. Holm, S. Koujak, S. Subramaniam, J. Vallon-Christersson, H. Olsson, T. Su, L. Memeo, T. Ludwig, S.P. Ethier, M. Krogh, M. Szabolcs, V.V. Murty, J. Isola, H. Hibshoosh, R. Parsons, A. Borg, Recurrent gross mutations of the PTEN tumor suppressor gene in breast cancers with deficient DSB repair, *Nat. Genet.* 40 (2008) 102-107. <https://doi.org/10.1038/ng.2007.39>.
- [21] S.L. Carter, A.C. Eklund, I.S. Kohane, L.N. Harris, Z. Szallasi, A signature of chromosomal instability inferred from gene expression profiles predicts clinical outcome in multiple human cancers, *Nat. Genet.* 38 (2006) 1043-1048. <https://doi.org/10.1038/ng1861>.
- [22] L. Zhang, B. Jiang, N. Zhu, M. Tao, Y. Jun, X. Chen, Q. Wang, C. Luo, Mitotic checkpoint kinase Mps1/TTK predicts prognosis of colon cancer patients and regulates tumor proliferation and differentiation via PKCalpha/ERK1/2 and PI3K/Akt pathway. *Med. Oncol.* 37 (2019) 5. <https://doi.org/10.1007/s12032-019-1320-y>
- [23] Y. Ling, X. Zhang, Y. Bai, P. Li, C. Wei, T. Song, Z. Zheng, K. Guan, Y. Zhang, B.

Zhang, X. Liu, R.Z. Ma, C. Cao, H. Zhong, Q. Xu, Overexpression of Mps1 in colon cancer cells attenuates the spindle assembly checkpoint and increases aneuploidy, *Biochem. Biophys. Res. Commun.* 450 (2014) 1690-1695. <https://doi.org/10.1016/j.bbrc.2014.07.071>.

[24] Q. Zhou, J. Ren, J. Hou, G. Wang, L. Ju, Y. Xiao, Y. Gong, Co-expression network analysis identified candidate biomarkers in association with progression and prognosis of breast cancer. *J. Cancer Res. Clin. Oncol.* 145 (2019) 2383-2396. <https://doi.org/10.1007/s00432-019-02974-4>.

[25] J. Tang, M. Lu, Q. Cui, D. Zhang, D. Kong, X. Liao, J. Ren, Y. Gong, G. Wu, Overexpression of ASPM, CDC20, and TTK Confer a Poorer Prognosis in Breast Cancer Identified by Gene Co-expression Network Analysis. *Front Oncol.* 9 (2019) 310. <https://doi.org/10.3389/fonc.2019.00310>.

[26] Z. Hu, C. Fan, D.S. Oh, J.S. Marron, X. He, B.F. Qaqish, C. Livasy, L.A. Carey, E. Reynolds, L. Dressler, A. Nobel, J. Parker, M.G. Ewend, L.R. Sawyer, J. Wu, Y. Liu, R. Nanda, M. Tretiakova, A. Ruiz Orrico, D. Dreher, J.P. Palazzo, L. Perreard, E. Nelson, M. Mone, H. Hansen, M. Mullins, J.F. Quackenbush, M.J. Ellis, O.I. Olopade, P.S. Bernard, C.M. Perou, The molecular portraits of breast tumors are conserved across microarray platforms, *BMC Genomics.* 7 (2006) 96. <https://doi.org/10.1186/1471-2164-7-96>.

[27] J. Daniel, J. Coulter, J.H. Woo, K. Wilsbach, E. Gabrielson, High levels of the Mps1 checkpoint protein are protective of aneuploidy in breast cancer cells, *Proc. Natl Acad. Sci. U. S. A.* 108 (2011) 5384-5389. <https://doi.org/10.1073/pnas.1007645108>.

[28] Feng, H.; Gu, Z. Y.; Li, Q.; Liu, Q. H.; Yang, X. Y.; Zhang, J. J. Identification of

significant genes with poor prognosis in ovarian cancer via bioinformatical analysis. *J. Ovarian res.* 12 (2019) 35. <https://doi.org/10.1186/s13048-019-0508-2>.

[29] R. Miao, H. Luo, H. Zhou, G. Li, D. Bu, X. Yang, X. Zhao, H. Zhang, S. Liu, Y. Zhong, Z. Zou, Y. Zhao, K. Yu, L. He, X. Sang, S. Zhong, J. Huang, Y. Wu, R.A. Miksad, S.C. Robson, C. Jiang, Y. Zhao, H. Zhao, Identification of prognostic biomarkers in hepatitis B virus-related hepatocellular carcinoma and stratification by integrative multi-omics analysis, *J. Hepatol.* 61 (2014) 840-849. <https://doi.org/10.1016/j.jhep.2014.05.025>.

[30] Y. Xie, A. Wang, J. Lin, L. Wu, H. Zhang, X. Yang, X. Wan, R. Miao, X. Sang, H. Zhao, Mps1/TTK: a novel target and biomarker for cancer, *J. Drug Target.* 25 (2017) 112-118. <https://doi.org/10.1080/1061186X.2016.1258568>.

[31] X. Liu, W. Liao, Q. Yuan, Y. Ou, J. Huang, TTK activates Akt and promotes proliferation and migration of hepatocellular carcinoma cells, *Oncotarget*, 6 (2015) 34309-34320. <https://doi.org/10.18632/oncotarget.5295>.

[32] T. Thykjaer, C. Workman, M. Kruhoffer, K. Demtroder, H. Wolf, L.D. Andersen, C.M. Frederiksen, S. Knudsen, T.F. Orntoft, Identification of gene expression patterns in superficial and invasive human bladder cancer, *Cancer Res.* 61 (2001) 2492-2499. <https://cancerres.aacrjournals.org/content/61/6/2492.long>.

[33] B.P. Kaistha, T. Honstein, V. Mueller, S. Bielak, M. Sauer, R. Kreider, M. Fassan, A. Scarpa, C. Schmees, H. Volkmer, T.M. Gress, M. Buchholz, Key role of dual specificity kinase TTK in proliferation and survival of pancreatic cancer cells, *Brit. J. Cancer.* 111 (2014) 1780-1787. <https://doi.org/10.1038/bjc.2014.460>.

- [34] L. Bie, G. Zhao, P. Cheng, G. Rondeau, S. Porwollik, Y. Ju, X.Q. Xia, M. McClelland, The accuracy of survival time prediction for patients with glioma is improved by measuring mitotic spindle checkpoint gene expression, *PLoS One*. 6 (2011) e25631. <https://doi.org/10.1371/journal.pone.0025631>.
- [35] B.A. Tannous, M. Kerami, P.M. Van der Stoop, N. Kwiatkowski, J. Wang, W. Zhou, A.F. Kessler, G. Lewandrowski, L. Hiddingh, N. Sol, T. Lagerweij, L. Wedekind, J.M. Niers, M. Barazas, R.J.A. Nilsson, D. Geerts, P.C.D.W. Hamer, C. Hagemann, W.P. Vandertop, O. Van Tellingen, D.P. Noske, N.S. Gray, T. Wuerdinger, Effects of the Selective MPS1 Inhibitor MPS1-IN-3 on Glioblastoma Sensitivity to Antimitotic Drugs, *JNCI J. Natl. Cancer Inst.* 105 (2013) 1322-1331. <https://doi.org/10.1093/jnci/djt168>.
- [36] U.B. Maachani, T. Kramp, R. Hanson, S. Zhao, O. Celiku, U. Shankavaram, R. Colombo, N.J. Caplen, K. Camphausen, A. Tandle, Targeting MPS1 Enhances Radiosensitization of Human Glioblastoma by Modulating DNA Repair Proteins, *Mol. Cancer Res.* 13 (2015) 852-862. <https://doi.org/10.1158/1541-7786.MCR-14-0462-T>.
- [37] D. Cimini, Merotelic kinetochore orientation, aneuploidy, and cancer, *Biochim. Biophys. Acta*. 1786 (2008) 32-40. <https://doi.org/10.1016/j.bbcan.2008.05.003>.
- [38] M. Schmidt, Y. Budirahardja, R. Klompaker, R. H. Medema, Ablation of the spindle assembly checkpoint by a compound targeting Mps1. *Embo Rep.* 6 (2005) 866-872. <https://doi.org/10.1038/sj.embor.7400483>
- [39] Santaguida, S.; Tighe, A.; D'Alise, A. M.; Taylor, S. S.; Musacchio, A. Reversine: Dissecting the role of MPS1 in chromosome biorientation and the spindle checkpoint through the small molecule inhibitor reversine. *J. Cell Biol.* 190 (2010) 73-87. <https://doi.org/10.1083/jcb.201001036>
- [40] S. Wang, M. Zhang, D. Liang, W. Sun, C. Zhang, M. Jiang, J. Liu, J. Li, C. Li, X.

Yang, X. Zhou, Molecular design and anticancer activities of small-molecule monopolar spindle 1 inhibitors: A Medicinal chemistry perspective. *Eur. J. Med. Chem.* 175 (2019) 247-268. <https://doi.org/10.1016/j.ejmech.2019.04.047>

[41] J.R. Riggs, J. Elsner, D. Cashion, D. Robinson, L. Tehrani, M. Nagy, K. Fultz, R. Krishna Narla, X. Peng, T. Tran, A. Kulkarni, S. Bahmanyar, K. Condroski, B. Pagarigan, G. Fenalti, L. LeBrun, K. Leftheris, D. Zhu, J. Boylan, Design and optimization leading to an orally active TTK protein kinase inhibitor with robust single agent efficacy, *J. Med. Chem.* 62 (2019) 4401-4410. <https://doi.org/10.1021/acs.jmedchem.8b01869>.

[42] J.R. Riggs, M. Nagy, J. Elsner, P. Erdman, D. Cashion, D. Robinson, R. Harris, D. Huang, L. Tehrani, G. Deyanat-Yazdi, R.K. Narla, X. Peng, T. Tran, L. Barnes, T. Miller, J. Katz, Y. Tang, M. Chen, M.F. Moghaddam, S. Bahmanyar, B. Pagarigan, S. Delker, L. LeBrun, P.P. Chamberlain, A. Calabrese, S.S. Canan, K. Leftheris, D. Zhu, J.F. Boylan, The Discovery of a Dual TTK Protein Kinase/CDC2-Like Kinase (CLK2) Inhibitor for the Treatment of Triple Negative Breast Cancer Initiated from a Phenotypic Screen, *J. Med. Chem.* 60 (2017) 8989-9002. <https://doi.org/10.1021/acs.jmedchem.7b01223>.

[43] N. Kwiatkowski, N. Jelluma, P. Filippakopoulos, M. Soundararajan, M.S. Manak, M. Kwon, H.G. Choi, T. Sim, Q.L. Deveraux, S. Rottmann, D. Pellman, J.V. Shah, G.J.P.L. Kops, S. Knapp, N.S. Gray, Small-molecule kinase inhibitors provide insight into Mps1 cell cycle function, *Nat. Chem. Biol.* 6 (2010) 359-368. <https://doi.org/10.1038/nchembio.345>.

[44] Y. Liu, Y. Lang, N.K. Patel, G. Ng, R. Laufer, S.W. Li, L. Edwards, B. Forrest, P.B. Sampson, M. Feher, F. Ban, D.E. Awrey, I. Beletskaya, G. Mao, R. Hodgson, O. Plotnikova, W. Qiu, N.Y. Chirgadze, J.M. Mason, X. Wei, D.C. Lin, Y. Che, R. Kiarash, B.

Madeira, G.C. Fletcher, T.W. Mak, M.R. Bray, H.W. Pauls, The Discovery of Orally Bioavailable Tyrosine Threonine Kinase (TTK) Inhibitors: 3-(4-(heterocycl)phenyl)-1H-indazole-5-carboxamides as Anticancer Agents, *J. Med. Chem.* 58 (2015) 3366-3392. <https://doi.org/10.1021/jm501740a>.

[45] V. K. Schulze, Klar, U.; Kosemund, D.; Wengner, A. M.; Siemeister, G.; Stockigt, D.; Neuhaus, R.; Lienau, P.; Bader, B.; Pechtl, S.; Holton, S. J.; Briem, H.; Marquardt, T.; Schirok, H.; Jautelat, R.; Bohlmann, R.; Nguyen, D.; Fernandez-Montalvan, A. E.; Bomer, U.; Eberspaecher, U.; Bruning, M.; Dohr, O.; Raschke, M.; Kreft, B.; Mumberg, D.; Ziegelbauer, K.; Brands, M.; von Nussbaum, F.; Koppitz, M. Treating Cancer by Spindle Assembly Checkpoint Abrogation: Discovery of Two Clinical Candidates, BAY 1161909 and BAY 1217389, Targeting MPS1 Kinase. *J. Med. Chem.* 2020 ASAP. <https://doi.org/10.1021/acs.jmedchem.9b02035>.

[46] A.M. Wengner, G. Siemeister, M. Koppitz, V. Schulze, D. Kosemund, U. Klar, D. Stoeckigt, R. Neuhaus, P. Lienau, B. Bader, S. Pechtl, M. Raschke, A.-L. Frisk, O. von Ahsen, M. Michels, B. Kreft, F. von Nussbaum, M. Brands, D. Mumberg, K. Ziegelbauer, Novel Mps1 Kinase Inhibitors with Potent Antitumor Activity, *Mol. Cancer Ther.* 15 (2016) 583-592. <https://doi.org/10.1158/1535-7163.mct-15-0500>.

[47] J.M. Mason, X. Wei, G.C. Fletcher, R. Kiarash, R. Brokx, R. Hodgson, I. Beletskaya, M.R. Bray, T.W. Mak, Functional characterization of CFI-402257, a potent and selective Mps1/TTK kinase inhibitor, for the treatment of cancer, *Proc. Natl. Acad. Sci. U. S. A.* 114 (2017) 3127-3132. <https://doi.org/10.1073/pnas.1700234114>.

[48] H.L. Woodward, P. Innocenti, K.J. Cheung, A. Hayes, J. Roberts, A.T. Henley, A. Faisal, G.W. Mak, G. Box, I.M. Westwood, N. Cronin, M. Carter, M. Valenti, A. De Haven Brandon, L. O'Fee, H. Saville, J. Schmitt, R. Burke, F. Broccatelli, R.L.M. van

Montfort, F.I. Raynaud, S.A. Eccles, S. Linardopoulos, J. Blagg, S. Hoelder, Introduction of a Methyl Group Curbs Metabolism of Pyrido[3,4- d]pyrimidine Monopolar Spindle 1 (MPS1) Inhibitors and Enables the Discovery of the Phase 1 Clinical Candidate N(2)-(2-Ethoxy-4-(4-methyl-4 H-1,2,4-triazol-3-yl)phenyl)-6-methyl-N(8)-neopentylpyrido[3,4- d]pyrimidine-2,8-diamine (BOS172722), *J. Med. Chem.* 61 (2018) 8226-8240. <https://doi.org/10.1021/acs.jmedchem.8b00690>.

[49] L. Yu, M. Huang, T. Xu, L. Tong, X.E. Yan, Z. Zhang, Y. Xu, C. Yun, H. Xie, K. Ding, X. Lu, A structure-guided optimization of pyrido[2,3-d]pyrimidin-7-ones as selective inhibitors of EGFR(L858R/T790M) mutant with improved pharmacokinetic properties, *Eur. J. Med. Chem.* 126 (2017) 1107-1117. <https://doi.org/10.1016/j.ejmech.2016.12.006>.

[50] T. Xu, T. Peng, X. Ren, L. Zhang, L. Yu, J. Luo, Z. Zhang, Z. Tu, L. Tong, Z. Huang, X. Lu, M. Geng, H. Xie, J. Ding, K. Ding, C5-substituted pyrido[2,3-d]pyrimidin-7-ones as highly specific kinase inhibitors targeting the clinical resistance-related EGFR T790M mutant, *Med. Chem. Comm.* 6 (2015) 1693-1697. <https://doi.org/10.1039/c5md00208g>.

[51] Q. Xun, Z. Zhang, J. Luo, L. Tong, M. Huang, Z. Wang, J. Zou, Y. Liu, Y. Xu, H. Xie, Z.C. Tu, X. Lu, K. Ding, Design, Synthesis, and Structure-Activity Relationship Study of 2-Oxo-3,4-dihydropyrimido[4,5- d]pyrimidines as New Colony Stimulating Factor 1 Receptor (CSF1R) Kinase Inhibitors, *J. Med. Chem.* 61 (2018) 2353-2371. <https://doi.org/10.1021/acs.jmedchem.7b01612>.

[52] We failed to purchase the reliable TTK kinase testing kit after querying multiple potential suppliers. We also contacted several major kinase service companies including

DiscoverX (San Diego) and Invitrogen (Thermo Fisher) et al., unfortunately they do not provide the TTK kinase inhibition service (only provide the binding assay).

[53] M.A. Fabian, W.H. Biggs, 3rd, D.K. Treiber, C.E. Atteridge, M.D. Azimioara, M.G. Benedetti, T.A. Carter, P. Ciceri, P.T. Edeen, M. Floyd, J.M. Ford, M. Galvin, J.L. Gerlach, R.M. Grotzfeld, S. Herrgard, D.E. Insko, M.A. Insko, A.G. Lai, J.M. Lelias, S.A. Mehta, Z.V. Milanov, A.M. Velasco, L.M. Wodicka, H.K. Patel, P.P. Zarrinkar, D.J. Lockhart, A small molecule-kinase interaction map for clinical kinase inhibitors, *Nat. Biotechnol.* 23 (2005) 329-336. <https://doi.org/10.1038/nbt1068>.

[54] J. Shen, T. Zhang, S.J. Zhu, M. Sun, L. Tong, M. Lai, R. Zhang, W. Xu, R. Wu, J. Ding, C.H. Yun, H. Xie, X. Lu, K. Ding, Structure-Based Design of 5-Methylpyrimidopyridone Derivatives as New Wild-Type Sparing Inhibitors of the Epidermal Growth Factor Receptor Triple Mutant (EGFR(L858R/T790M/C797S)), *J. Med. Chem.* 62 (2019) 7302-7308. <https://doi.org/10.1021/acs.jmedchem.9b00576>.

[55] R. Colombo, M. Caldarelli, M. Mennecozzi, M.L. Giorgini, F. Sola, P. Cappella, C. Perrera, S.R. Depaolini, L. Rusconi, U. Cucchi, N. Avanzi, J.A. Bertrand, R.T. Bossi, E. Pesenti, A. Galvani, A. Isacchi, F. Colotta, D. Donati, J. Moll, Targeting the Mitotic Checkpoint for Cancer Therapy with NMS-P715, an Inhibitor of MPS1 Kinase, *Cancer Res.* 70 (2010) 10255-10264. <https://doi.org/10.1158/0008-5472.can-10-2101>.

[56] L. Hewitt, A. Tighe, S. Santaguida, A.M. White, C.D. Jones, A. Musacchio, S. Green, S.S. Taylor, Sustained Mps1 activity is required in mitosis to recruit O-Mad2 to the Mad1-C-Mad2 core complex, *J. Cell Biol.* 190 (2010) 25-34. <https://doi.org/10.1083/jcb.201002133>.

- [57] M. Jemaa, L. Galluzzi, O. Kepp, L. Senovilla, M. Brands, U. Boemer, M. Koppitz, P. Lienau, S. Prechtel, V. Schulze, G. Siemeister, A.M. Wengner, D. Mumberg, K. Ziegelbauer, A. Abrieu, M. Castedo, I. Vitale, G. Kroemer, Characterization of novel MPS1 inhibitors with preclinical anticancer activity, *Cell Death Differ.* 20 (2013) 1532-1545. <https://doi.org/10.1038/cdd.2013.105>.
- [58] K.D. Tardif, A. Rogers, J. Cassiano, B.L. Roth, D.M. Cimbora, R. McKinnon, A. Peterson, T.B. Douce, R. Robinson, I. Dorweiler, T. Davis, M.A. Hess, K. Ostanin, D.I. Papac, V. Baichwal, I. McAlexander, J.A. Willardsen, M. Saunders, H. Christophe, D.V. Kumar, D.A. Wettstein, R.O. Carlson, B.L. Williams, Characterization of the Cellular and Antitumor Effects of MPI-0479605, a Small-Molecule Inhibitor of the Mitotic Kinase Mps1, *Mol. Cancer Ther.* 10 (2011) 2267-2275. <https://doi.org/10.1158/1535-7163.mct-11-0453>.
- [59] N. Kwiatkowski, N. Jelluma, P. Filippakopoulos, M. Soundararajan, M.S. Manak, M. Kwon, H.G. Choi, T. Sim, Q.L. Deveraux, S. Rottmann, D. Pellman, J.V. Shah, G.J. Kops, S. Knapp, N.S. Gray, Small-molecule kinase inhibitors provide insight into Mps1 cell cycle function, *Nat. Chem. Biol.* 6 (2010) 359-368. <https://doi.org/10.1038/nchembio.345>.
- [60] V.M. Stucke, H.H.W. Silljé, L. Arnaud, E.A. Nigg, Human Mps1 kinase is required for the spindle assembly checkpoint but not for centrosome duplication, *EMBO J.* 21 (2002) 1723-1732. <https://doi.org/10.1093/emboj/21.7.1723>.
- [61] A. Abrieu, L.M. Jaulin, J.A. Kahana, M. Peter, A. Castro, S. Vigneron, T. Lorca, D.W. Cleveland, J. C. Labbé, Mps1 Is a Kinetochore-Associated Kinase Essential for the

Vertebrate Mitotic Checkpoint, *Cell*. 106 (2001) 83-93.
[https://doi.org/10.1016/S0092-8674\(01\)00410-X](https://doi.org/10.1016/S0092-8674(01)00410-X).

[62] M.W. Schmidt, K.K. Baldridge, J.A. Boatz, S.T. Elbert, M.S. Gordon, J.H. Jensen, S. Koseki, N. Matsunaga, K.A. Nguyen, S. Su, T.L. Windus, M. Dupuis, J. John A. Montgomery, General Atomic and Molecular Electronic Structure System, *J. Comput. Chem.* 14 (1993) 1347-1363. <https://doi.org/10.1002/jcc.540141112>.

[63] C.I. Bayly, P. Cieplak, W.D. Cornell, P.A. Kollman, A Well-Behaved Electrostatic Potential Based Method Using Charge Restraints for Deriving Atomic Charges: The RESP Model, *The J. Phy. Chem.* 97 (1993) 10269-10280.
<https://doi.org/10.1021/j100142a004>.

[64] B. Hess, C. Kutzner, D. van der Spoel, E. Lindahl, GROMACS 4: Algorithms for Highly Efficient, Load-Balanced, and Scalable Molecular Simulation, *J. Chem. Theory Comput.* 4 (2008) 435-447. <https://doi.org/10.1021/ct700301q>.

[65] B.R. Miller, 3rd, T.D. McGee, Jr., J.M. Swails, N. Homeyer, H. Gohlke, A.E. Roitberg, MMPBSA.py: An Efficient Program for End-State Free Energy Calculations, *J. Chem. Theory Comput.* 8 (2012) 3314-3321. <https://doi.org/10.1021/ct300418h>.

[66] Z. Wang, Y. Zhang, D.M. Pinkas, A.E. Fox, J. Luo, H. Huang, S. Cui, Q. Xiang, T. Xu, Q. Xun, D. Zhu, Z. Tu, X. Ren, R.A. Brekken, A.N. Bullock, G. Liang, K. Ding, X. Lu, Design, Synthesis, and Biological Evaluation of 3-(Imidazo[1,2-a]pyrazin-3-ylethynyl)-4-isopropyl-N-(3-((4-methylpiperazin-1-yl)methyl)-5-(trifluoromethyl)phenyl)benzamide as a Dual Inhibitor of Discoidin Domain Receptors 1 and 2, *J. Med. Chem.* 61 (2018) 7977-7990.

<https://doi.org/10.1021/acs.jmedchem.8b01045>.

Journal Pre-proof

HIGHLIGHTS

- A series of pyrido[2, 3-*d*]pyrimidin-7(8*H*)-ones were designed and synthesized as new selective orally bioavailable TTK inhibitors.
- Compounds **5o** exhibited high potency against TTK while was obvious less potent for the majority of a panel of 402 wild-type kinases investigated.
- Compounds **5o** induced chromosome missegregation and aneuploidy, and suppressed proliferation of a panel of human cancer cells.
- Compounds **5o** demonstrated good oral pharmacokinetic properties.
- Combination therapy of **5o** with paclitaxel displayed promising *in vivo* efficacy against the HCT-116 xenograft model in nude mice.

Declaration of Interest Statement

The authors declare no interest of conflict.

Ke Ding

On behalf of all authors listed in this manuscript

2020-3-19

Journal Pre-proof